

# Strong disorder renormalization group study of aperiodic quantum Ising chains

Fleury J. Oliveira Filho, Maicon S. Faria, and André P. Vieira

Instituto de Física da USP, São Paulo, SP, Brazil

**Abstract.** We employ an adaptation of a strong-disorder renormalization-group technique in order to analyze the ferro-paramagnetic quantum phase transition of Ising chains with aperiodic but deterministic couplings under the action of a transverse field. In the presence of marginal or relevant geometric fluctuations induced by aperiodicity, for which the critical behavior is expected to depart from the Onsager universality class, we derive analytical and asymptotically exact expressions for various critical exponents (including the correlation-length and the magnetization exponents, which are not easily obtainable by other methods), and shed light onto the nature of the ground state structures in the neighborhood of the critical point. The main results obtained by this approach are confirmed by finite-size scaling analyses of numerical calculations based on the free-fermion method.

## 1. Introduction

Quantum phase transitions differ from thermal transitions in that they happen at zero temperature, induced by quantum fluctuations ultimately inherent to all physical systems. As these transitions occur at zero temperature, they can be verified even in one-dimensional systems, which are especially sensitive to the effects of both quantum and geometric fluctuations, being thus ideal laboratories for the study of exotic phenomena associated with the presence of disorder.

Arguably the simplest spin model to undergo a quantum phase transition is the quantum Ising chain, described by the Hamiltonian

$$H = -\frac{1}{2} \sum_{j=1}^N J_j \sigma_j^x \sigma_{j+1}^x - \frac{1}{2} \sum_{j=1}^N h_j \sigma_j^z, \quad (1)$$

in which the  $\sigma^{x,z}$  are Pauli matrices,  $J_j > 0$  represents a ferromagnetic bond between the longitudinal components of the spins at sites  $j$  and  $j+1$ , and  $h_j$  denotes a transverse field acting on the spin at site  $j$ . In the uniform limit ( $J_j \equiv J$ ,  $h_j \equiv h > 0$ ), there is a quantum phase transition at  $h = J$ , between a ferromagnetic phase dominated by the nearest-neighbor bonds  $J$ , and a paramagnetic phase, dominated by the fields  $h$ . In this case, the model corresponds to the extreme anisotropy limit of the two-dimensional Ising model. Indeed, the quantum transition at  $h = J$  belongs to the Onsager universality class, whose paradigm is precisely the thermal transition of the two-dimensional Ising model.

In the presence of disorder represented by randomly chosen couplings  $J_j$  and  $h_j$ , the model in Eq. 1 exhibits surprising behavior. By extending a strong-disorder real-space renormalization group (SDRG) scheme introduced by Ma, Dasgupta, and Hu [1, 2] to study the random Heisenberg chain, Fisher [3, 4] was able to show that the nature of the quantum transition is fundamentally changed with respect to that of the uniform limit, being now characterized by a brutal distinction between average and typical behavior of various physical quantities, such as correlation functions. At criticality, there is a modification of the dynamic relation between length and time scales, which assumes an activated form (*à la* Arrhenius), in contrast with the usual power law. Sufficiently close to criticality, there are Griffiths phases [5], in which some thermodynamic properties are still singular. Fisher also provided exact calculations of a series of other properties for the random system, many of which are not known in the uniform limit, such as the scaling form for the magnetization as a function of an ordering field at the critical point.

Partially similar effects are verified in the presence of aperiodic but deterministic couplings. This kind of aperiodicity is inspired by analogy with quasicrystals [6], which exhibit symmetries forbidden by traditional crystallography, corresponding to projections of high-dimensional Bravais lattices on low-dimensional subspaces. In one spatial dimension, aperiodic couplings can be defined from sequences of letters obtained from substitution or inflation rules, such as the one associated with the Fibonacci sequence,  $a \rightarrow ab$ ,  $b \rightarrow a$ . Iteration of this rule yields a sequence  $abaababa \dots$  with no

characteristic period. By associating different letters with different bond values  $J_a$  and  $J_b$  (or with different field values  $h_a$  and  $h_b$ ) one obtains an aperiodic quantum Ising chain. Any aperiodic sequence induces geometric fluctuations gauged by a wandering exponent  $\omega$ , which describes the growth of these fluctuations as the chain length increases. A value of  $\omega = \frac{1}{2}$  would mimic the geometric fluctuations induced by random couplings.

For aperiodic quantum Ising chains, there are exact results obtained by RG treatments, unrelated to the SDRG scheme, and valid at the critical point [7, 8, 9]. These results allow the inference of the relation between length and time scales, and show that aperiodic sequences characterized by a wandering exponent  $\omega = \frac{1}{2}$  induce, at the critical point, effects analogous to those produced by randomness. Additionally, they confirm the validity of a heuristic criterion formulated by Luck [10] in order to gauge the effects of aperiodicity on ferromagnetic phase transitions. According to this criterion, aperiodicity is relevant, *i.e.* it is capable of changing the critical behavior of the quantum Ising chain, whenever it is associated with a wandering exponent  $\omega > 0$ . The marginal case  $\omega = 0$  may lead to nonuniversal critical behavior, dependent on the coupling values.

In the present paper, we adapt the SDRG scheme to study the critical behavior of quantum Ising chains with aperiodic couplings. We show that this adaptation allows us to investigate the system both at the critical point and in its neighborhood, and to obtain presumably exact analytical results for a series of critical exponents, such as those associated with the bulk magnetization, the critical correlations, and the correlation length, which are not easily accessible via other methods. This allows a comparison with numerical results obtained for some of these exponents by Iglói *et al.* from a mapping of the quantum Ising chain to a free-fermion problem [11, 12]. We note that essentially the same SDRG approach has been employed to study the scaling form of the entanglement entropy in aperiodic quantum Ising chains, although only at the critical point [13, 14].

This paper is organized as follows. In Section 2 we review the SDRG approach introduced to deal with the random quantum Ising chain, as well as the associated low-energy physics. In Section 3 we introduce the kind of aperiodic structures in which we focus on this paper, as well as the notion of geometric fluctuations, discussing their connection with the Harris-Luck criterion for the relevance of aperiodicity to the critical behavior of the quantum Ising chain. Section 4 presents our extension of the SDRG approach to deal with aperiodic quantum Ising chains with couplings chosen from a family of aperiodic sequences whose geometric fluctuations can be tuned from irrelevant to relevant. In Section 5 we discuss the behavior of quantum Ising chains with couplings following Rudin-Shapiro sequences, whose geometric fluctuations mimic those associated with random couplings. The final section presents our concluding remarks.

## 2. Random quantum Ising chains and the strong-disorder RG approach

The random quantum Ising chain corresponds to the extremely anisotropic limit of the McCoy-Wu model [15, 16], and its very interesting low-temperature properties have been elucidated by Fisher [3, 4], who argued that an adaptation of the strong-disorder renormalization group (SDRG) approach of Ma, Dasgupta and Hu [1, 2] yields asymptotically exact results for various physical quantities.

The basic idea of the SDRG scheme is the iterative elimination of high-energy degrees of freedom, associated with locally strong couplings. For sufficiently strong randomness, in which there are very few strong couplings and many weak couplings, this is easily defined. In a finite chain, there is always a strongest coupling. If this coupling is a field, say  $h_2$ , most likely the neighboring bonds  $J_1$  and  $J_2$  are much weaker, and the spin  $\sigma_2$  will tend to align with the transverse field, giving negligible contributions to magnetic properties. If we are interested in the low-energy behavior, the spin  $\sigma_2$ , along with the field  $h_2$  and the bonds  $J_1$  and  $J_2$ , can be eliminated from the system. Nevertheless, virtual excitations will induce an effective coupling between the  $x$  components of the neighboring spins  $\sigma_1$  and  $\sigma_3$ , given, up to second order in perturbation theory, by

$$\tilde{J}_1 = \frac{J_1 J_2}{h_2}. \quad (2)$$

If the strongest coupling is a bond, say  $J_2$ , the spins  $\sigma_1$  and  $\sigma_2$  that it connects are most likely under the action of much weaker fields  $h_1$  and  $h_2$ , and thus will tend to respond, at low energies, as a single effective spin, under the action of an effective transverse field created by virtual excitations and given, again up to second order, by

$$\tilde{h}_1 = \frac{h_1 h_2}{J_2}. \quad (3)$$

The bond  $J_2$  and the fields  $h_1$  and  $h_2$ , along with the spins  $\sigma_1$  and  $\sigma_2$ , are then replaced by the effective spin, with an effective magnetic moment, acted on by the field  $\tilde{h}_1$ .

In any case, the overall energy scale is reduced, since both effective couplings  $\tilde{h}_1$  and  $\tilde{J}_1$  are always weaker than any of the original couplings. As the transformations described above are iterated, this leads to a renormalization of the probability distributions of both bonds and fields, as well as lengths and magnetic moments. The fixed-point distributions can be found in closed form [4, 17], and from these many low-energy physical properties can be derived. The nature of the ground state is strongly modified by the presence of disorder. While there is still a well-defined critical point, which corresponds to Pfeuty's exact result [18],

$$\overline{\ln h_i} = \overline{\ln J_i},$$

the critical relation between length ( $l$ ) and energy ( $\Omega$ ) scales departs from the power law valid in the uniform chain, having now the activated form

$$\Omega \sim \exp\left(-\sqrt{l/l_0}\right),$$

where  $l_0$  is some nonuniversal length scale. Most strikingly, in the neighborhood of the critical point the model is still gapless and the dynamic scaling behavior follows

$$\Omega \sim l^{-z(\delta)},$$

in which  $z(\delta)$  is a dynamical exponent dependent on the distance to the critical point, measured by  $\delta \sim \overline{\ln h_i} - \overline{\ln J_i}$ . This gapless noncritical regime arises from the existence of rare but arbitrarily large regions of spins which, due to statistical fluctuations, are locally in the “wrong” phase as compared to the whole chain, yielding the so-called Griffiths singularities [5].

Interestingly, the above results seem to be asymptotically valid not only for strong disorder, but for any amount of randomness present in the system. The reason is most easily seen at criticality, where the probability distributions of effective couplings become more and more singular around the origin, rendering the perturbative expressions for the effective couplings essentially exact. In the following sections, we show that also in the presence of relevant aperiodic modulations it is possible to obtain asymptotically exact results, although the nature of the ground state turns out to be quite distinct from that of the random case.

### 3. Aperiodic sequences and the Harris-Luck criterion

Substitution rules defining aperiodic sequences have the general form

$$\{a_i \rightarrow w_i, \quad i \in \{1, 2, \dots, n\},$$

in which  $w_i$  is a “word” formed by letters in the set  $\{a_i\}$ . The sequence is built by iteratively applying the rule to an initial letter. For instance, the celebrated Fibonacci sequence is obtained by applying the rule

$$\begin{cases} a \rightarrow ab \\ b \rightarrow a \end{cases}$$

to an initial letter  $a$ .

Various properties of the resulting infinite sequence (obtained after an infinite number of iterations of the rule) are related to the substitution matrix

$$\mathbb{M} = \begin{pmatrix} f_{11} & f_{12} & \cdots & f_{1n} \\ f_{21} & f_{22} & \cdots & f_{2n} \\ \vdots & \vdots & \ddots & \vdots \\ f_{n1} & f_{n2} & \cdots & f_{nn} \end{pmatrix},$$

in which  $f_{ij}$  denotes the number of letters  $a_i$  in the word  $w_j$ . For instance, the length of the sequence after  $k$  iterations of the substitution rule is asymptotically given by

$$N_k \sim \zeta_1^k,$$

$\zeta_1 > 0$  being the largest eigenvalue of  $\mathbb{M}$ . Also, the  $i$ th entry of the corresponding eigenvector (normalized so as the sum of all entries equals unity) gives the relative frequency  $d_i$  of the different letters in the infinite sequence.

For the purposes of the present paper, the most relevant property derived from the substitution matrix are the fluctuations of the relative frequency of a letter, after  $k$  iterations of the rule, with respect to that of the infinite sequence. These fluctuations are explicitly defined as

$$g_k^{(i)} = \left| N_k^{(i)} - d_i N_k \right|,$$

where  $N_k^{(i)}$  denotes the number of letters  $a_i$  after  $k$  iterations of the substitution rule. It can be shown that  $g_k^{(i)}$ , for all  $i$ , is asymptotically governed by the second largest eigenvalue (in absolute value) of  $\mathbb{M}$ ,

$$g_k^{(i)} \sim |\zeta_2|^k \equiv N_k^\omega,$$

in which

$$\omega \equiv \frac{\ln |\zeta_2|}{\ln \zeta_1}$$

is the so-called wandering exponent of the aperiodic sequence. A negative value of  $\omega$  indicates that fluctuations are bounded, and become negligible as the length of the sequence becomes larger and larger. On the other hand, a positive  $\omega$  leads to unbounded fluctuations, as in the case of a sequence built from independently and randomly distributed letters, for which  $\omega = \frac{1}{2}$ . Finally, the marginal case of  $\omega = 0$  usually leads to fluctuations which grow logarithmically with the sequence length.

When couplings in a ferromagnetic model are chosen in a nonperiodic fashion, the Harris-Luck heuristic criterion [10, 19] makes use of the concept of the fluctuations of those couplings in a length scale defined by the correlation length to point out under which conditions aperiodicity changes the critical behavior with respect to that of the uniform system. In the case of a quantum Ising chain with bonds chosen from some aperiodic sequence, such fluctuations are proportional to the  $g_k^{(i)}$  defined above, and the criterion states that aperiodicity will be relevant, *i.e.* the critical behavior will be changed, whenever the wandering exponent satisfies

$$\omega \geq 1 - \frac{1}{\nu} = 0, \quad (4)$$

in which  $\nu = 1$  is the correlation-length critical exponent of the Onsager universality class.

In the following section, we analyze the effects of bonds chosen from a family of aperiodic sequences with wandering exponents ranging from  $\omega = -1$  to  $\omega \rightarrow 1$ .

#### 4. A family of aperiodic sequences

Consider the family of aperiodic sequences generated by the substitution rule [20]

$$\begin{cases} a \rightarrow ab^k \\ b \rightarrow a \end{cases}, \quad b^k \equiv \underbrace{bb \cdots b}_{k \text{ letters}} \quad (5)$$

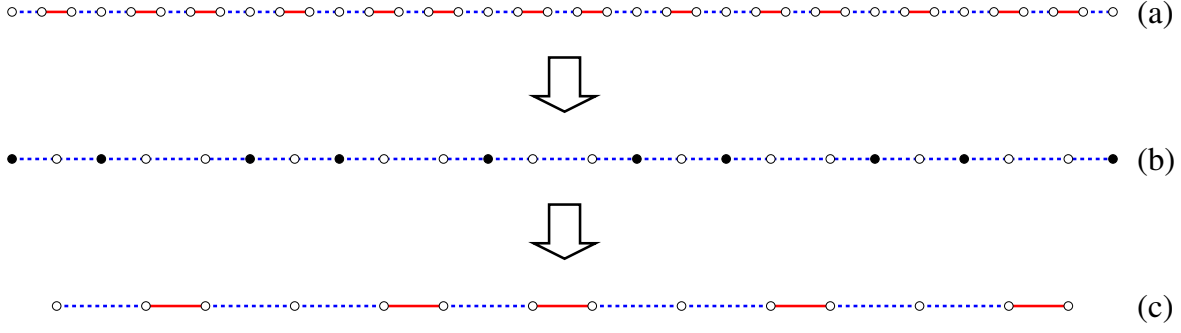


Figure 1: Renormalization-group transformation as applied to the Fibonacci chain. The original chain is depicted in (a), with weak  $J_a$  bonds indicated by dashed (blue) lines and strong  $J_b$  bonds by solid (red) lines; spins sit on the open circles, under the action of the original transverse field  $h$ . After the spins connected by strong bonds are joined, the chain takes the form shown in (b), with open circles now denoting effective fields  $\tilde{h}$  and solid circles representing original fields  $h$ . Decimation of the spins under the action of  $h$  leads to the sequence of effective couplings shown in (c), which again corresponds to a Fibonacci chain.

with  $k$  a positive integer, so that  $k = 1$  corresponds to the Fibonacci sequence, illustrated in Fig. 1(a). The substitution matrix has eigenvalues

$$\zeta_k^\pm = \frac{1}{2} \pm \frac{1}{2} \sqrt{1 + 4k},$$

and thus the wandering exponent,

$$\omega_k = \frac{\ln |\zeta_k^-|}{\ln \zeta_k^+} = \frac{\ln k}{\ln \zeta_k^+} - 1, \quad (6)$$

is a monotonically increasing function of  $k$ , with  $\omega_1 = -1$ ,  $\omega_2 = 0$ ,  $\omega_3 = 0.317\dots$ , etc. According to the Harris-Luck criterion, we thus expect that aperiodicity is relevant for  $k \geq 3$ , with  $k = 2$  representing a marginal case.

The sequences generated by Eq. 5 contain clusters of  $k$  letters  $b$ , separated by clusters of 1 or  $k + 1$  letters  $a$ . In order to implement a strong-disorder RG treatment of the corresponding quantum Ising chain, we have to calculate the effective bonds and fields associated with those clusters. Although we start with a uniform field, the RG scheme will generate different effective fields for different clusters, and this will be taken into account in the discussion below.

We first look at the case of  $n$  spins  $\sigma_i$  ( $i = 1, 2, \dots, n$ ) under the action of a field  $h_0$ , forming with spins  $\sigma_l$  and  $\sigma_r$  a cluster connected by  $n + 1$  bonds  $J \ll h_0$ ; see Fig. 2(a). Furthermore, suppose that the fields  $h_l$  and  $h_r$  acting on  $\sigma_l$  and  $\sigma_r$  are small compared to  $h_0$ . Physically, one expects that the  $n$  spins in the cluster tend to line up with the field  $h_0$ , and thus can be decimated out of the system. Applying perturbation theory up to order  $n + 1$  leads to the conclusion that fluctuations of the cluster induce an effective

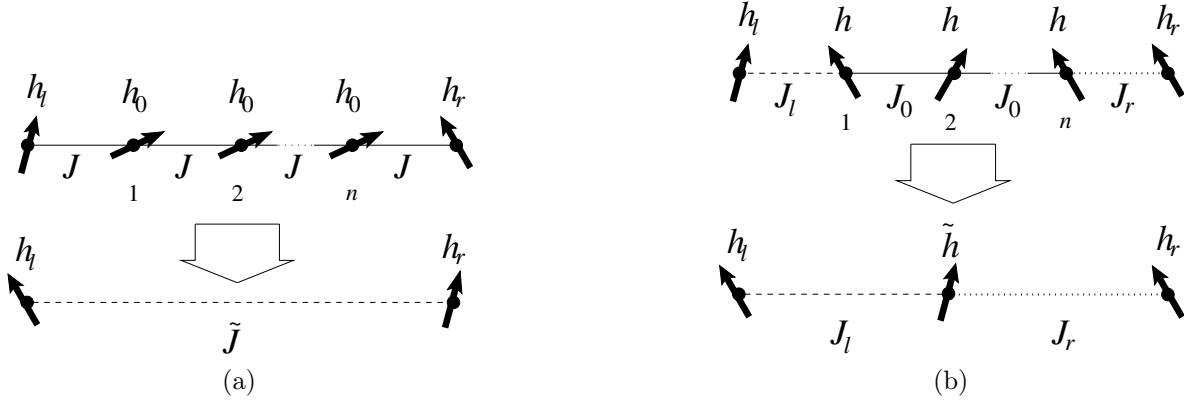


Figure 2: Renormalization of couplings and decimation of spins in the aperiodic quantum Ising chain. (a) Elimination of spins connected by  $n$  neighboring strong fields  $h_0$ . (b) Formation of an effective spin from a cluster of  $n$  spins connected by strong bonds  $J_0$ .

coupling

$$\tilde{J} = \frac{J^{n+1}}{h_0^n} \quad (7)$$

between  $\sigma_l$  and  $\sigma_r$ .

A more delicate situation corresponds to a cluster of  $n$  spins connected by strong bonds  $J_0$ , while the field  $h$  acting on each of the  $n$  spins, as well as the bonds  $J_l$  and  $J_r$  to the rest of the chain, are much smaller; see Fig. 2(b). However, this can be easily dealt with by resorting to a duality transformation [21], which interchanges the roles of bonds and fields. In the transformed space, the situation is precisely the one of the previous paragraph, so that the result can be immediately written down. At low energies, the  $n$  spins behave as a single magnetic moment, under the action of an effective field

$$\tilde{h} = \frac{h^n}{J_0^{n-1}}, \quad (8)$$

with an effective magnetic moment

$$\tilde{\mu} = n\mu, \quad (9)$$

$\mu$  being the magnetic moment of each of the  $n$  spins.

Getting back to the sequences generated by Eq. 5, suppose we look at intermediate values of the field, so that  $J_a \ll h \ll J_b$ . (The case  $J_a \gg J_b$  leads to a renormalized chain in which the roles of weak and strong bonds are interchanged, as long as the system is sufficiently close to criticality. Thus, there is no loss of generality in assuming  $J_b \gg J_a$ .) At energy scales  $\Omega$  such that  $h < \Omega < J_b$ , Eqs. 8 and 9 imply that each cluster of  $k+1$  spins connected by bonds  $J_b$  behaves as a single magnetic moment, under the action of an effective field

$$\tilde{h} = \frac{h^{k+1}}{J_b^k}, \quad (10)$$

with an effective magnetic moment

$$\tilde{\mu} = (k + 1) \mu. \quad (11)$$

As  $\tilde{h} < h$ , and  $J_a < h$ , the largest coupling is now provided by the original field  $h$ , as illustrated in Fig. 1(b) for the case of the Fibonacci chain. Further reducing the energy scale, so that  $J_a < \Omega < h$ , the clusters of  $k + 1$  bonds  $J_a$ , containing  $k$  spins under the action of the field  $h$ , can be decimated out, leaving effective bonds

$$\tilde{J}_a = \frac{J_a^{k+1}}{h^k}, \quad (12)$$

as shown in Fig. 1(c). All original fields  $h$  are decimated in this step, so that all active spins at this energy scale are under the action of the same field  $\tilde{h}$ . Now the largest couplings in the chain are provided by the remaining clusters of isolated  $J_a$  bonds, which we can interpret as effective bonds

$$\tilde{J}_b = J_a, \quad (13)$$

since with this choice the sequence of effective bonds exactly reproduces the original sequence. Equations 10 through 13 define an RG step.

In general, there is no guarantee that the effective couplings satisfy the condition  $\tilde{J}_a < \tilde{h} < \tilde{J}_b$ , which is required to iterate the RG procedure. However, we shall assume that the condition is satisfied, and explore the consequences. We first introduce a change in notation, rewriting the RG equations as

$$J_a^{(j+1)} = \frac{[J_a^{(j)}]^{k+1}}{[h^{(j)}]^k}, \quad J_b^{(j+1)} = J_a^{(j)}, \quad (14)$$

$$h^{(j+1)} = \frac{[h^{(j)}]^{k+1}}{[J_b^{(j)}]^k}, \quad \mu^{(j+1)} = (k + 1) \mu^{(j)}, \quad (15)$$

in which  $J_a^{(j)}$ ,  $J_b^{(j)}$ ,  $h^{(j)}$  and  $\mu^{(j)}$  represent the values of the parameters after  $j$  iterations of the RG procedure, with  $J_a^{(0)} \equiv J_a$ ,  $J_b^{(0)} \equiv J_b$ ,  $h^{(0)} \equiv h$ , and  $\mu^{(0)} = 1$ . Next, we define the ratios

$$r^{(j)} = \frac{h^{(j)}}{J_b^{(j)}} \quad \text{and} \quad s^{(j)} = \frac{J_a^{(j)}}{h^{(j)}}, \quad (16)$$

which both remain smaller than unity as long as the condition  $J_a^{(j)} < h^{(j)} < J_b^{(j)}$  is fulfilled. From Eqs. 14 and 15 we obtain recursion relations for the ratios,

$$r^{(j+1)} = \frac{[r^{(j)}]^k}{s^{(j)}} \quad \text{and} \quad s^{(j+1)} = \frac{[s^{(j)}]^{k+1}}{[r^{(j)}]^k},$$

which can be written in matrix form by taking the logarithm of the previous equations, yielding

$$\begin{pmatrix} \ln r^{(j+1)} \\ \ln s^{(j+1)} \end{pmatrix} = \begin{pmatrix} k & -1 \\ -k & k+1 \end{pmatrix} \begin{pmatrix} \ln r^{(j)} \\ \ln s^{(j)} \end{pmatrix}. \quad (17)$$

Defining

$$|v_j\rangle = \begin{pmatrix} \ln r^{(j)} \\ \ln s^{(j)} \end{pmatrix} \quad \text{and} \quad \mathbb{T}_k = \begin{pmatrix} k & -1 \\ -k & k+1 \end{pmatrix}, \quad (18)$$

and expressing the matrix  $\mathbb{T}_k$  as  $\mathbb{T}_k = \mathbb{U}_k \mathbb{D}_k \mathbb{U}_k^{-1}$ , in which the diagonal matrix  $\mathbb{D}_k$  consists of the eigenvalues of  $\mathbb{T}_k$  and the columns of the matrix  $\mathbb{U}_k$  contain the corresponding right eigenvectors, we can rewrite Eq. 17 as

$$|u_{j+1}\rangle \equiv \mathbb{U}_k^{-1} |v_{j+1}\rangle = \mathbb{D}_k \mathbb{U}_k^{-1} |v_j\rangle \equiv \mathbb{D}_k |u_j\rangle,$$

from which we readily obtain

$$|u_j\rangle = \mathbb{D}_k^j |u_0\rangle \quad \Rightarrow \quad |v_j\rangle = \mathbb{U}_k \mathbb{D}_k^j \mathbb{U}_k^{-1} |v_0\rangle. \quad (19)$$

The eigenvalues of the matrix  $\mathbb{T}_k$  are related to the eigenvalues of the substitution matrix by

$$\lambda_k^\pm = k + \zeta_k^\pm = (\zeta_k^\pm)^2,$$

while the matrix  $\mathbb{U}_k$  can be written as

$$\mathbb{U}_k = \begin{pmatrix} 1 & 1 \\ -\zeta_k^+ & -\zeta_k^- \end{pmatrix}.$$

Using the above results, we can invert  $\mathbb{U}_k$  and expand Eq. 19 to obtain

$$\ln r^{(j)} = \frac{1}{\zeta_k^+ - \zeta_k^-} \left[ -(\lambda_k^+)^j \alpha_k^- + (\lambda_k^-)^j \alpha_k^+ \right] \quad (20)$$

and

$$\ln s^{(j)} = \frac{1}{\zeta_k^+ - \zeta_k^-} \left[ (\lambda_k^+)^j \zeta_k^+ \alpha_k^- - (\lambda_k^-)^j \zeta_k^- \alpha_k^+ \right], \quad (21)$$

with

$$\alpha_k^\pm = \zeta_k^\pm \ln r^{(0)} + \ln s^{(0)}.$$

We thus see that the behavior of  $r^{(j)}$  and  $s^{(j)}$  for  $j \gg 1$  is in general dominated by the largest eigenvalue of  $\mathbb{T}_k$ ,  $\lambda_k^+ > \lambda_k^- > 0$ . If  $\alpha_k^-$ , which enters the coefficient of  $(\lambda_k^+)^j$  in both  $\ln r^{(j)}$  and  $\ln s^{(j)}$ , is positive, we asymptotically have  $\ln r^{(j)} \ll 0$  and  $\ln s^{(j)} \gg 0$ , and thus the effective fields are much smaller than the effective bonds. This corresponds to the ferromagnetic phase. Conversely, if  $\alpha_k^-$  is negative, the asymptotic behavior corresponds to  $\ln r^{(j)} \gg 0$  and  $\ln s^{(j)} \ll 0$ , the effective fields are much larger than the effective bonds, and the system is in the paramagnetic phase. The critical point must then correspond to the condition  $\alpha_k^- = 0$ , which, in terms of the original parameters, leads to a critical field

$$h_{\text{crit}} = J_a^{\frac{1}{1-\zeta_k^-}} J_b^{-\frac{\zeta_k^-}{1-\zeta_k^-}} = J_a^{d_a} J_b^{d_b}, \quad (22)$$

in which  $d_a$  and  $d_b = 1 - d_a$  can be shown to be the fractions of letters  $a$  and  $b$  in the infinite sequence produced by Eq. 5. This last result agrees with the exact result derived by Pfeuty [18] for the critical condition of the quantum Ising chain. That the

approximate RG equations used here are able to lead to the exact result in Eq. 22 must be related to the fact that the recurrence relations 10, 12 and 13 preserve the dual symmetry of the quantum Ising chain.

It is also useful to determine the effective lengths of the various couplings as the RG scheme is iterated. We follow Fisher [4] and assume that fields and bonds share lengths evenly, so that the initial bonds have lengths  $\ell_a^{(0)} = \ell_b^{(0)} = \frac{1}{2}$  and the initial field has length  $\ell_h^{(0)} = \frac{1}{2}$ . From Eqs. 14 and 15, and by looking at Fig. 1, we see that these lengths satisfy recursion relations which can be written in matrix form as

$$\begin{pmatrix} \ell_a^{(j+1)} \\ \ell_b^{(j+1)} \\ \ell_h^{(j+1)} \end{pmatrix} = \begin{pmatrix} k+1 & 0 & k \\ 1 & 0 & 0 \\ 0 & k & k+1 \end{pmatrix} \begin{pmatrix} \ell_a^{(j)} \\ \ell_b^{(j)} \\ \ell_h^{(j)} \end{pmatrix} \equiv \mathbb{S}_k \begin{pmatrix} \ell_a^{(j)} \\ \ell_b^{(j)} \\ \ell_h^{(j)} \end{pmatrix}.$$

Thus, all effective lengths grow asymptotically with the largest eigenvalue of the matrix  $\mathbb{S}_k$ . It turns out that the eigenvalues of  $\mathbb{S}_k$  are 1,  $\lambda_k^-$  and  $\lambda_k^+$ , so that

$$\ell_a^{(j)} \sim \ell_b^{(j)} \sim \ell_h^{(j)} \sim (\lambda_k^+)^j. \quad (23)$$

In the following subsections, we analyze the consequences of the previous expressions for the behavior of the system both at the critical point and in its neighborhood.

#### 4.1. Properties at the critical point

The recursion relations 14 and 15 can be iterated indefinitely at the critical point. As then  $\alpha_k^- = 0$ , the behavior of the ratios  $r^{(j)}$  and  $s^{(j)}$  is determined only by the smallest eigenvalue  $\lambda_k^-$  of the matrix  $\mathbb{T}_k$ ,

$$\ln r^{(j)} = \frac{\alpha_k^+}{\zeta_k^+ - \zeta_k^-} (\lambda_k^-)^j \quad \text{and} \quad \ln s^{(j)} = -\frac{\alpha_k^+ \zeta_k^-}{\zeta_k^+ - \zeta_k^-} (\lambda_k^-)^j. \quad (24)$$

Precisely at the critical point, there are exact real-space RG calculations [7, 8, 9] that provide information on the dynamic scaling between energy levels and length scales. These can be used to gauge the reliability of the SDRG approach developed here.

*4.1.1. Irrelevant aperiodicity.* For the Fibonacci chain, which corresponds to  $k = 1$ , we have  $\lambda_k^- \simeq 0.382$ , so that both  $r^{(j)}$  and  $s^{(j)}$  asymptotically approach unity. This means that the perturbative recursion relations become poorer and poorer approximations as the iterations proceed, suggesting at the same time, in agreement with known results (see [7] and references therein), that the critical behavior should correspond to that of the uniform chain. In other words, Fibonacci modulations are irrelevant for the critical behavior of the quantum Ising chain, and the relation between energy and length scales at criticality follows the usual dynamical scaling form

$$\Omega \sim \ell^{-z},$$

with a dynamic exponent  $z = 1$ .

4.1.2. *Marginal aperiodicity.* For  $k = 2$ , we have  $\lambda_k^- = 1$ , so that both  $r^{(j)}$  and  $s^{(j)}$  remain constant along the iterations, being expressed in terms of the original bonds as

$$r^{(j)} = \left(\frac{J_a}{J_b}\right)^{d_a} \quad \text{and} \quad s^{(j)} = \left(\frac{J_a}{J_b}\right)^{1-d_a},$$

so that the ratio between the effective bonds is constant,

$$\rho^{(j)} \equiv \frac{J_a^{(j)}}{J_b^{(j)}} = r^{(j)} s^{(j)} = \frac{J_a}{J_b} \equiv \rho.$$

This corresponds to a line of critical points, associated with different values of the ratio  $\rho = J_a/J_b$ , and gives rise to a nonuniversal dynamic exponent  $z$ , as already known for other aperiodic sequences [7, 8, 9], and for quantum Ising chains with correlated disorder [22]. Indeed, if we use the values of the strong bonds at each step of the RG procedure to estimate the gaps  $\Omega_j$  between different energy levels, we get

$$\Omega_j \sim J_b^{(j)} = J_a^{(j-1)} = \frac{J_a^{(j-1)}}{J_b^{(j-1)}} J_b^{(j-1)} = \rho J_b^{(j-1)} = \rho^j J_b,$$

while Eq. 23 leads to a characteristic length

$$\ell_j \sim \ell_b^{(j)} \sim (\lambda_2^+)^j = 4^j.$$

Expressing  $j$  in terms of  $\ell_j$ , we then obtain the dynamic scaling form

$$\Omega_j \sim \ell_j^{-z(\rho)}, \quad (25)$$

with a dynamic exponent

$$z(\rho) = -\frac{\ln \rho}{\ln 4}. \quad (26)$$

As in the case of the quantum spin- $\frac{1}{2}$  XX chain with marginal aperiodic bonds [23, 24], the dynamic exponent coming out of the SDRG approach corresponds to the leading term in the  $\rho \ll 1$  expansion of an exact result which can be obtained by other methods [8, 9, 25]. In the present case, the exact result turns out to be

$$z_{\text{ex}}(\rho) = \frac{\ln(\rho^{1/2} + \rho^{-1/2})}{2}, \quad (27)$$

which can be obtained from the corresponding result for the quantum Ising chain with bonds chosen from the period-doubling sequence generated by the substitution rule

$$\begin{cases} A \rightarrow AB \\ B \rightarrow AA \end{cases}.$$

Distributing couplings  $J_A$  and  $J_B \gg J_A$  according to the above sequence, and applying an intermediate field  $h$ , the SDRG approach leads to a sequence of bonds  $J_a$  and  $J_b$  given by the rule in Eq. 5 with  $k = 2$ . At criticality, these bonds are related to the original ones via

$$J_a = \frac{J_A^{5/3}}{J_B^{2/3}}, \quad J_b = J_A,$$

so that

$$\frac{J_a}{J_b} = \left( \frac{J_A}{J_B} \right)^{2/3}.$$

Thus, the exact result for the period-doubling chain [8, 9] translates into Eq. 27, which, for  $\rho \ll 1$ , clearly reduces to Eq. 26.

*4.1.3. Relevant aperiodicity.* For  $k \geq 3$ , the wandering exponent  $\omega_k$  is positive. According to the Harris-Luck criterion, this corresponds to relevant aperiodicity.

It is easy to check that, under the condition  $k \geq 3$ ,  $\lambda_k^-$  is larger than unity. Since we start with  $r^{(0)} < 1$  and  $s^{(0)} < 1$ , we have  $\alpha_k^+ < 0$ , and Eq. 24 implies that both  $r^{(j)}$  and  $s^{(j)}$  become arbitrarily close to zero as the RG scheme proceeds. This means that the perturbative recursion relations become asymptotically exact, as does the RG treatment itself. This is analogous to what happens for the random quantum Ising chain [3, 4]. It is then not surprising that the activated dynamic scaling form

$$\Omega_j \sim \exp[-(\ell_j/\ell_\rho)^\omega], \quad (28)$$

with  $\ell_\rho \sim |\ln \rho|^{-1/\omega}$  a length scale that depends on the original couplings, is exactly reproduced by the SDRG treatment, as it can be readily checked from Eqs. 14, 15, 22, and 23. Thus, the dynamic exponent is formally infinite. This result is analogous to what is verified for the critical spin- $\frac{1}{2}$  XXZ chain with relevant aperiodic bonds [23, 24].

Notice that  $\omega$  here plays the role of the “tunneling” exponent  $\psi$  in the random quantum Ising chain [26], which owes its name to the need of high-energy virtual excitations in order to flip spin clusters.

#### 4.2. The neighborhood of the critical point

In order to study the system in the neighborhood of the critical point, we set

$$h = h_{\text{crit}}(1 - \delta), \quad |\delta| \ll 1,$$

with  $\delta$  measuring the distance to criticality. It is clear from the previous discussion that, for  $\delta \neq 0$ , the RG process has to be interrupted whenever the condition

$$\max \{ \ln r^{(j)}, \ln s^{(j)} \} = 0 \quad (29)$$

is reached, which happens for a value of  $j$  we denote by  $j_\delta$ . By using Eqs. 20 and 21, together with the initial values

$$r^{(0)} = \frac{h}{J_b} = \rho^{d_a}(1 - \delta) \quad \text{and} \quad s^{(0)} = \frac{J_a}{h} = \rho^{d_b}(1 - \delta)^{-1},$$

in which we again make use of the ratio  $\rho = J_a/J_b$  between the original bond values, we can show that for  $|\delta| \ll 1$  the condition in Eq. 29 leads to

$$j_\delta = \frac{\ln |\delta|}{\ln(\lambda_k^-/\lambda_k^+)} + c\rho \sim \frac{\ln |\delta|}{\ln(\lambda_k^-/\lambda_k^+)}, \quad (30)$$

$c$  being a constant which is different in the paramagnetic ( $\delta < 0$ ) and in the ferromagnetic ( $\delta > 0$ ) phases.

This last result allows us to obtain analytical expressions for critical exponents, as discussed below. Of course, the reported results are not valid for  $k = 1$ , where the critical behavior corresponds to that of the uniform chain.

*4.2.1. The paramagnetic phase.* The paramagnetic phase is characterized by the fact that after  $j_\delta$  iterations all effective bonds are smaller than the effective fields. Thus, the length of the largest effective bonds at this point of the RG process provides an estimate of the correlation length.

Substituting Eq. 30 into Eq. 23, we obtain

$$\xi \sim \ell_b^{(j_\delta)} \sim (\lambda_k^+)^{j_\delta} \sim |\delta|^{-\nu},$$

with a correlation-length exponent

$$\nu = \frac{\ln \lambda_k^+}{\ln \lambda_k^+ - \ln \lambda_k^-}. \quad (31)$$

As  $\lambda_k^\pm = (\zeta_k^\pm)^2$ , this last result can be rewritten as

$$\nu = \frac{1}{1 - \omega_k}. \quad (32)$$

We thus see that the correlation-length exponent at the aperiodic critical point saturates the Harris-Luck criterion in the form

$$\nu \geq \frac{1}{1 - \omega}, \quad (33)$$

for all sequences in the family generated by the substitution rule in Eq. 5. In particular, for the marginal case of  $k = 2$  we recover the exact result  $\nu = 1$  [8, 9]. We note that Eq. 33 is analogous to the Chayes bound for the correlation length critical exponent in the presence of disorder [27].

We can also study the behavior of the energy gap as a function of  $\delta$ . From the discussion in Subsection 4.1, we see that the energy gap vanishes at the critical point, since  $\Omega_j \rightarrow 0$  as  $j \rightarrow \infty$ ; see Eqs. 25 and 28. On the other hand, in the paramagnetic phase the value of the effective field  $h^{(j)}$  for  $j = j_\delta$ , being much larger than any other effective coupling, yields an estimate of the energy gap between the ground state and the first excited state of the infinite chain. We thus have

$$\Omega(\delta) \sim h^{(j_\delta)} \sim |\delta|^{z(\rho)\nu},$$

for marginal aperiodicity ( $k = 2$ ), and,

$$\Omega(\delta) \sim h^{(j_\delta)} \sim \exp(-C|\delta|^{-\omega\nu}), \quad (34)$$

for relevant aperiodicity ( $C$  being a nonuniversal constant). The above expressions can be derived from the recursion relations in Eqs. 14 and 15, with the help of Eq. 30. Notice that  $\Omega(\delta) \rightarrow 0$  as  $\delta \rightarrow 0$ , but the noncritical gap is always finite, implying the absence of Griffiths singularities in the presence of aperiodic fluctuations generated by substitution rules [12, 25].

*4.2.2. The ferromagnetic phase.* In the ferromagnetic phase, after  $j_\delta$  iterations of the RG transformation the effective field becomes smaller than both effective bonds. An estimate of the average spontaneous magnetization is provided by the average magnetic moment of all the spins still active at this point of the RG procedure (*i.e.* those that have not been decimated under the action of strong local fields in the previous RG steps). Since the sequence of bonds remains invariant up to this point, the estimate is simply given by

$$m_x \sim n_{j_\delta} \mu^{(j_\delta)} \sim \frac{\mu^{(j_\delta)}}{\ell_{j_\delta}},$$

in which  $n_j$  is the fraction of active spins after  $j$  iterations of the RG transformation. From Eq. 15, we see that

$$\mu^{(j)} = (k+1)^j \mu_0,$$

yielding

$$m_x \sim \left( \frac{k+1}{\lambda_k^+} \right)^{j_\delta}.$$

Substituting Eq. 30 then leads to

$$m_x \sim \delta^\beta,$$

with a critical exponent

$$\beta = \frac{\ln(k+1) - \ln \lambda_k^+}{\ln \lambda_k^- - \ln \lambda_k^+}. \quad (35)$$

Notice that, if we follow Fisher [3, 4] and define at the critical point an exponent  $\phi$  relating the effective magnetic moment to the energy scale,

$$\mu^{(j)} \sim \left[ \ln \frac{\Omega_\rho}{\Omega_j} \right]^\phi,$$

where  $\Omega_\rho$  is a nonuniversal constant, we find

$$\beta = \nu (1 - \phi\psi),$$

just as for the random quantum Ising chain [26].

### 4.3. Critical correlation functions

Now we determine the asymptotic behavior of the pair correlation function associated with the order parameter,

$$C^{xx}(l) = \overline{\langle \sigma_i^x \sigma_{i+l}^x \rangle},$$

in which the bar denotes average over all lattice sites  $i$ . At criticality, this correlation function follows a power-law scaling form,

$$C^{xx}(l) \sim \frac{1}{l^\eta}.$$

In the uniform limit, and thus also for the Fibonacci chain, the exponent  $\eta$  takes the value  $\frac{1}{4}$  [28]. Below we calculate  $\eta$  for  $k \geq 2$ .

The elements associated with the strongest bonds  $J_b^{(j)}$  in each RG step are clusters containing  $k + 1$  spins. Each of these clusters, if decoupled from the rest of the chain, has a doubly degenerate ground state (in the absence of a field), corresponding to all spins pointing along the  $+x$  or the  $-x$  direction. If we denote these states by  $|\Psi^\pm\rangle$ , it is clear that

$$\langle \Psi^\pm | \sigma_i^x | \Psi^\pm \rangle = \pm 1,$$

in which  $i$  labels the spins inside a given cluster.

Owing to the inflation symmetry associated with couplings generated by the substitution rule in Eq. 5, these clusters are either grouped into superclusters of  $k + 1$  clusters or are separated from each other by  $k + 1$  weak bonds  $J_a$ , as illustrated for  $k = 2$  in Fig. 3(a). The superclusters, on the other hand, are either grouped into “supersuperclusters” containing  $k + 1$  superclusters or isolated from each other by clusters and weak bonds, and so on. Thus, there appears a hierarchy of  $(k + 1)$ -spin clusters, yielding a self-similar structure of the correlation function, and leading to the appearance of characteristic distances where the correlation is particularly strong.

In order to analyze this structure, we recourse to the simplest approximation, in which we assume that spins appearing in the same cluster at some step of the RG scheme are maximally correlated, while the remaining correlations are negligible. Looking at Fig. 3(a), we see that, in the limit of a very large chain (where boundary effects can be ignored), the average correlation between spins separated by the distance  $l_0 \equiv \ell_b^{(0)} + \ell_h^{(0)} = 1$ , corresponding to the real distance between nearest-neighbor spins connected by a coupling  $J_b$ , is given by

$$C^{xx}(l_0) = \frac{1}{N} \times k \times \frac{N_b^{(0)}}{k} = \frac{N_b^{(0)}}{N},$$

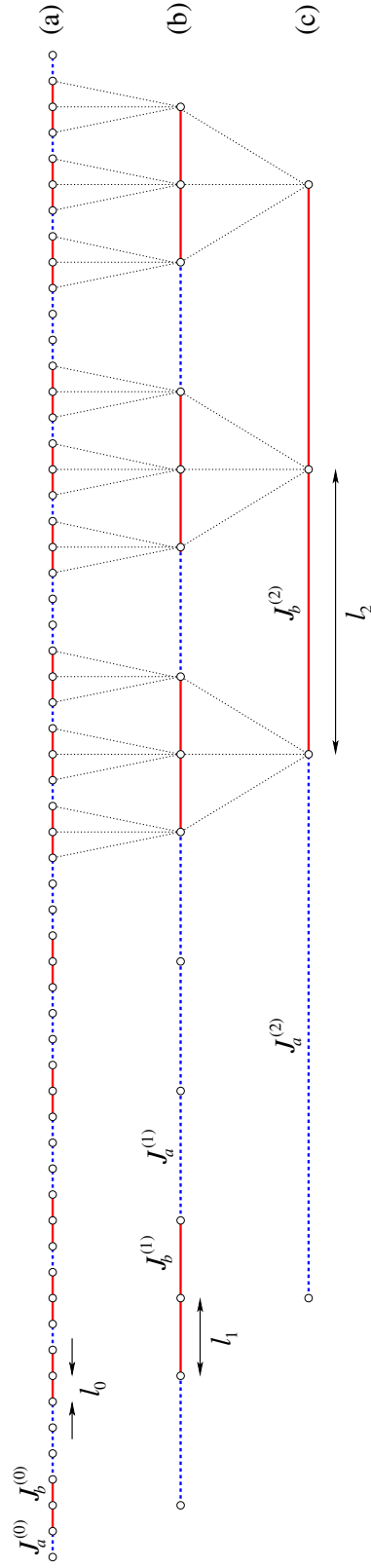
in which  $N$  is the total number of spins,  $N_b^{(0)}$  is the number of  $J_b$  bonds ( $\frac{1}{k}N_b^{(0)}$  being the number of clusters with  $k + 1$  spins), and the multiplicative  $k$  factor comes from the fact that in each cluster there are  $k$  pairs of spins separated by the distance  $l_0$ . In fact, we have

$$C^{xx}(l'_0) = \frac{k + 1 - g_0}{k} \times \frac{N_b^{(0)}}{N},$$

since in each cluster there are  $k + 1 - g_0$  pairs of spins separated by the distance  $l'_0 = g_0 l_0$ ,  $g_0 \in \{1, 2, \dots, k\}$ . However, the strongest correlation corresponds to the value  $g_0 = 1$ , coming from spins separated by the distance  $l'_0 = l_0$ .

From Fig. 3(b), we see that an estimate of the average correlation between spins separated the distance  $l_1 \equiv \ell_b^{(1)} + \ell_h^{(1)} = k + 1$  is given by

$$C^{xx}(l_1) = \left[ \frac{1}{N} \times k \times \frac{N_b^{(1)}}{k} \right] \times (k + 1) = (k + 1) \frac{N_b^{(1)}}{N},$$

Figure 3: Estimating correlation functions for the case  $k=2$ .

with  $N_b^{(1)}$  denoting the number of effective bonds  $J_b^{(1)}$  and the multiplicative factor  $k+1$  coming from the fact that each effective spin represents  $k+1$  real spins in this step of the hierarchy. Notice that inside each cluster there are in fact contributions to the average correlation between real spins separated by distances  $l'_1 = g_1 l_1 \pm g_0 l_0$ , where  $g_1 \in \{1, 2, \dots, k\}$  and  $g_0 \in \{0, 1, \dots, k\}$ . (However, these correlations are strongest for  $l'_1 = l_1$ .) Since  $l_1 - k l_0 = 1$ ,  $l_1 - (k-1) l_0 = 2$ ,  $\dots$ ,  $l_1 - l_0 = k$ , this gives corrections to the average correlations  $C^{xx}(l_0)$ ,  $C^{xx}(2l_0)$ ,  $\dots$ ,  $C^{xx}(kl_0)$  between spins separated by short distances in the real chain.

Figure 3(c) leads us to conclude that the average correlation between real spins separated by the distance  $l_2 \equiv \ell_b^{(2)} + \ell_h^{(2)} = k^2 + 3k + 1$  is approximately given by

$$C^{xx}(l_1) = \left[ \frac{1}{N} \times k \times \frac{N_b^{(2)}}{k} \right] \times (k+1)^2 = (k+1)^2 \frac{N_b^{(2)}}{N},$$

since now every effective spin represents  $(k+1)^2$  real spins. In fact, there are contributions to the average correlations between real spins separated by distances  $l'_2 = g_2 l_2 \pm g_1 l_1 \pm g_0 l_0$ , in which  $g_2 \in \{1, 2, \dots, k\}$  and  $g_1, g_0 \in \{0, 1, \dots, k\}$ . (Again, the strongest contribution comes from spins separated by the distance  $l'_2 = l_2$ .) Here there are corrections to correlations between spins separated by distances of the order of  $l_1$ , but not of the order of  $l_0$ , since  $l_2 - k l_1 - k l_0 = l_1$  corresponds to the minimum value of  $l'_2$ .

Generalizing the above discussion, there are strong correlations associated with distances around  $l_j \equiv \ell_b^{(j)} + \ell_h^{(j)} \sim (\lambda_k^+)^j$ , with

$$C^{xx}(l_j) = (k+1)^j \frac{N_b^{(j)}}{N},$$

$N_b^{(j)}$  being the number of effective bonds  $J_b^{(j)}$  in a chain with  $N \gg 1$  sites. Actually, there are contributions to correlations between real spins separated by distances

$$l'_j = g_j l_j \pm g_{j-1} l_{j-1} \pm \dots \pm g_0 l_0,$$

with  $g_j \in \{1, 2, \dots, k\}$  and  $g_{i \neq j} \in \{0, 1, \dots, k\}$ , so that the strongest contribution appears for  $l'_j = l_j$ , and the minimum value of  $l'_j$  is of the order of  $l_{j-1}$ . Thus, there are no corrections for correlations between spins separated by distances of the order of  $l_{j-2}$  and below.

Owing to the invariance of the sequence of effective bonds along the RG steps, the number of effective  $J_b^{(j)}$  bonds scales as

$$N_b^{(j)} \sim \frac{N}{l_j}.$$

It is then clear that we can estimate the long-distance scaling behavior of the average strong correlations as

$$C^{xx}(l_j) \sim \frac{(k+1)^j}{l_j} \sim \frac{1}{l_j^\eta},$$

with an exponent

$$\eta = 1 - \frac{\ln(k+1)}{\ln \lambda_k^+} = \frac{\beta}{\nu}. \quad (36)$$

This result is in contrast with the one obtained for the random quantum Ising chain, for which critical correlations decay with distance as  $C^{xx}(l) \sim l^{-2\beta/\nu}$  [4, 17], due to the probabilistic nature of cluster formation.

#### 4.4. Numerical calculations

The analytical results derived in the previous subsections can be checked by numerical calculations based on the well-known mapping of the quantum Ising chain onto a free-fermion system [29, 30]. Here we use the recipe described in Ref. [31]. The numerical work then involves diagonalizing matrices of order  $2L$  for chains containing  $L$  spins. As here we work with open boundary conditions, this corresponds to  $L - 1$  bonds.

When dealing with finite chains, we have to take into account that substitution rules produce aperiodic systems containing many different subsequences of the same length  $L - 1$ . We then have to perform a weighted average over all  $O(L)$  such subsequences, with weights given by the frequencies with which a given subsequence appears in the infinite sequence. For arbitrary  $L$ , in order to determine these frequencies we iterate the substitution rule until a very large sequence of size  $\mathcal{L}$  (with  $\mathcal{L}$  ranging from  $\sim 10^4$  to  $\sim 10^6$ ) is obtained. We then calculate the finite-size estimates of the corresponding frequencies, and extrapolate to infinite  $\mathcal{L}$  using standard algorithms [32]. In order to minimize fluctuations due to the discrete scale invariance exhibited by substitutional sequences, the number of bonds,  $L - 1$ , is always chosen to coincide with the length of the aperiodic sequences after an integer number of iterations of the substitution rule.

We work here in the so-called canonical ensemble of disorder, according to which we study the critical properties of the system by performing numerical calculations for a value of the transverse field corresponding to the critical field of the infinite sequence. The other possibility, which defines the microcanonical ensemble, would correspond to setting the transverse field to values calculated from the densities of letters  $a$  and  $b$  in each particular subsequence of finite length, which are usually distinct from the infinite-sequence value. It has been shown that the canonical ensemble yields the same critical exponents as exact and RG calculations [31].

The finite-size behavior of the bulk critical magnetization is described by

$$m_x(L) \sim L^{-\beta/\nu},$$

for systems of size  $L$ . Within the free-fermion approach, this scaling behavior can be checked by calculating magnetization profiles (i.e. local expectation values of the spin operators  $\sigma_l^x$ ,  $l = 1, 2, \dots, L$ ) in finite chains with prescribed boundary conditions [31]. Here we focus on fixed boundary conditions, corresponding to  $h_1 = 0$  and  $h_L = 0$ , and look at the resulting profiles when both end spins are in the state  $|\sigma_i^x\rangle = |+\rangle$ .

For  $k = 3$ , a case in which aperiodic modulations are relevant, we expect the SDRG prediction for  $\beta/\nu$  to be valid for any coupling ratio  $\rho = J_a/J_b$ . Of course for  $J_a/J_b$  close

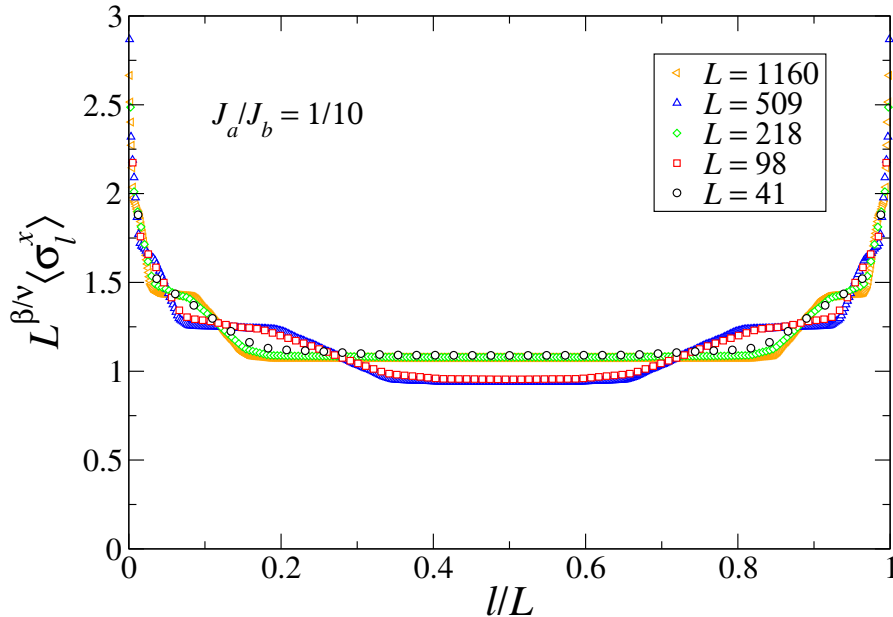


Figure 4: Rescaled magnetization profiles for  $k = 3$  at the critical point, for different chain lengths  $L$ . The values of the exponents  $\beta$  and  $\nu$  were set to their SDRG predictions, yielding  $\beta/\nu \simeq 0.169$ . Calculations were performed for fixed ends,  $\langle \sigma_1^x \rangle = \langle \sigma_L^x \rangle = +1$ , and the curves result from averaging over all distinct subsequences of length  $L$ , followed by mirror symmetrization around the position  $l = L/2$ .

to unity there will be a large crossover length  $L_\times$ , below which the system will appear uniform, and the SDRG result should be recovered only for  $L > L_\times$ , while for smaller values of  $\rho$  the SDRG should be evident even for relatively small chain lengths. This is confirmed by the free-fermion calculations, as shown in Fig. 4 for  $J_a/J_b = 1/10$ . Notice that the results for finite  $L$  ( $L$  between 41 and 1160) collapse onto two different master curves, depending on whether the subsequence size was produced after an odd or an even number of iterations of the substitution rule. This is related to the fact that the deviation of the number of letters  $a$  (or equivalently  $b$ ) with respect to the expectation value in the infinite sequence oscillates in sign between consecutive iterations of the substitution rule (the eigenvalue  $\zeta_2$  of the substitution matrix is negative). Furthermore, it should be noted that none of the master curves follows the conformal invariance prediction [33, 34]

$$m_x(l/L) = \langle \sigma_l^x \rangle \sim [L \sin(\pi l/L)]^{-\beta/\nu},$$

as expected from the strongly anisotropic scaling along the space and time directions implied by Eq. 28.

In the marginal case,  $k = 2$ , we only expect the SDRG predictions to be satisfied for coupling ratios approaching zero. Indeed, as shown in Fig. 5, a plot of the finite-size behavior of the bulk magnetization at criticality (estimated from the corresponding value in the middle of the chain) shows a clear change from the Onsager universality class to the strong-modulation behavior as the coupling ratio is reduced.

The behavior of the critical pair correlation function  $C^{xx}(l)$ , as obtained from the

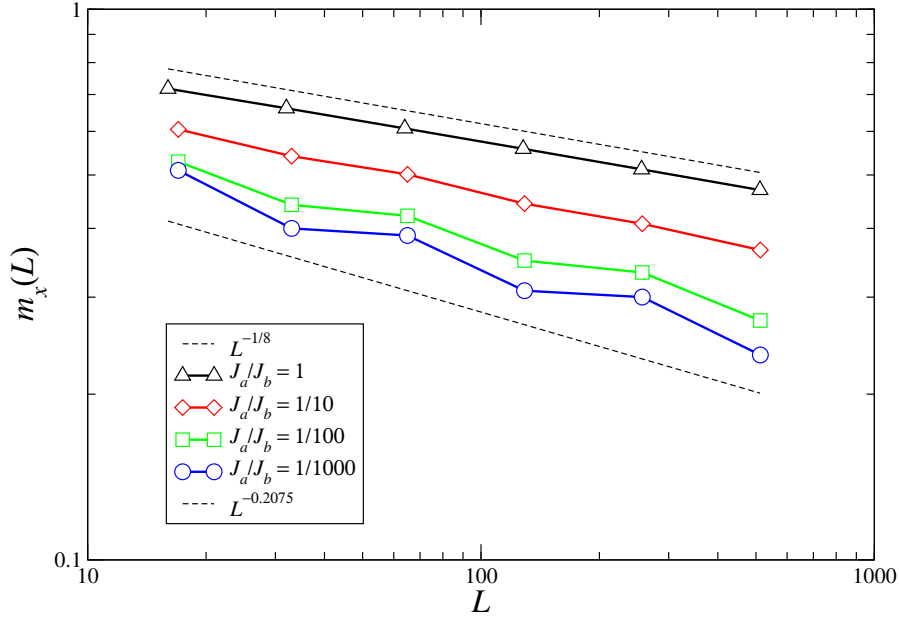


Figure 5: Critical bulk magnetization for  $k = 2$  as a function of the chain length  $L$ . The upper dashed curves correspond to the Onsager behavior  $L^{-\beta/\nu}$ , with  $\beta/\nu = 1/8$ , while the lower dashed curve indicates the SDRG prediction,  $\beta/\nu \simeq 0.2075$ .

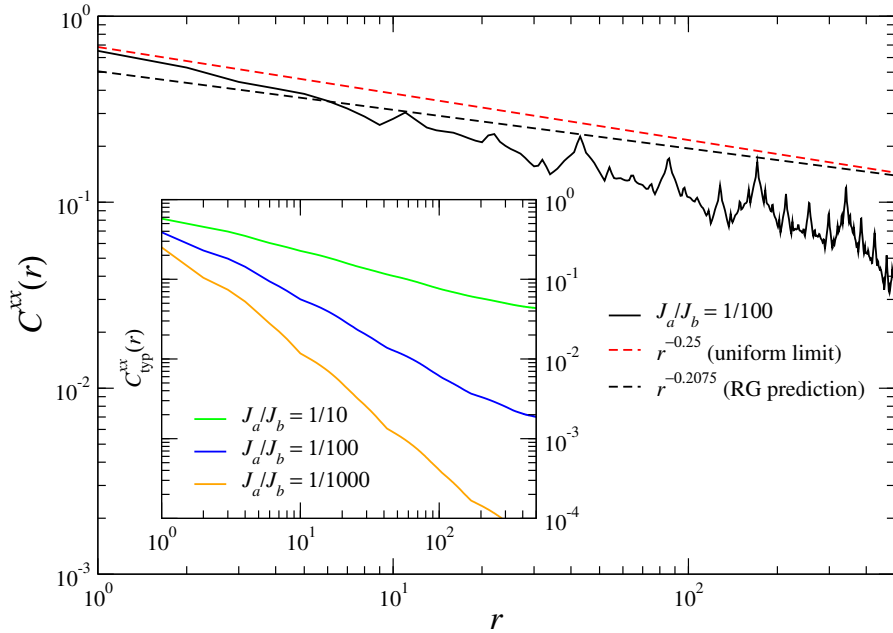


Figure 6: Main panel: Average pair correlation function versus spin separation for  $k = 2$ . The red dashed curve shows the Onsager behavior, while the black dashed curve indicates the SDRG prediction, which is valid at the characteristic distances where correlations are strong. Inset: Typical correlation function for various values of the coupling ratio.

free-fermion method, is illustrated in the main panel of Fig. 6 for  $k = 2$  and a small coupling ratio  $J_a/J_b = 1/100$ . Notice the existence of characteristic distances for which spins are strongly correlated, due to the presence of strong effective bonds, and of a ultrametric structure produced by the cluster hierarchy discussed in Subsection 4.3. The inset shows plots of the typical correlation, estimated by

$$C_{\text{typ}}^{xx}(l) \equiv \exp \left( \overline{\ln \langle \sigma_i^x \sigma_{i+l}^x \rangle} \right),$$

which exhibits nonuniversal behavior and a much smoother dependence on the spin separation  $l$ , confirming that, as in the random quantum Ising chain, there is a decoupling between average and typical behavior.

## 5. Rudin-Shapiro sequences

### 5.1. The four-letter sequence

The family of sequences analyzed in the previous section has the property that, at the criticality, there is only one type of spin cluster connected by strong bonds at a given step of the RG process. A more complex situation is produced by choosing bonds according to the four-letter Rudin-Shapiro (RS) sequence, generated by the substitution rule

$$\begin{cases} a \rightarrow ab \\ b \rightarrow ac \\ c \rightarrow db \\ d \rightarrow dc \end{cases} . \quad (37)$$

The associated substitution matrix has eigenvalues  $0, \pm\sqrt{2}$ , and  $2$ , so that the wandering exponent is  $\omega = \frac{1}{2}$ , the same produced by uncorrelated randomness. In the resulting infinite sequence all letters appear with the same frequency, and no clusters of repeated letters are present.

We choose couplings such that  $J_b = \rho J_a$ ,  $J_c = \rho^2 J_a$ , and  $J_d = \rho^3 J_a$ , with  $0 < \rho < 1$ . Based on Pfeuty's result [18], we anticipate a critical field

$$h_{\text{crit}} = \rho^{\frac{3}{2}} J_a,$$

so that, in order to look at the system in the neighborhood of the critical point, we focus on the condition  $J_d \ll J_c \ll h \ll J_b \ll J_a$ . At energy scales  $\Omega$  such that  $J_d < J_c < \Omega < h < J_b < J_a$ , all spin pairs connected by  $J_a$  or  $J_b$  bonds behave as single magnetic moments, whereas spins connected to their neighbors at both sides by only  $J_c$  or  $J_d$  bonds are effectively removed from the chain by the action of the transverse field; see Fig. 7(a). The resulting effective chain is composed of 6 different bonds and fields, whose values (in decreasing order of intensity), and those of the corresponding effective

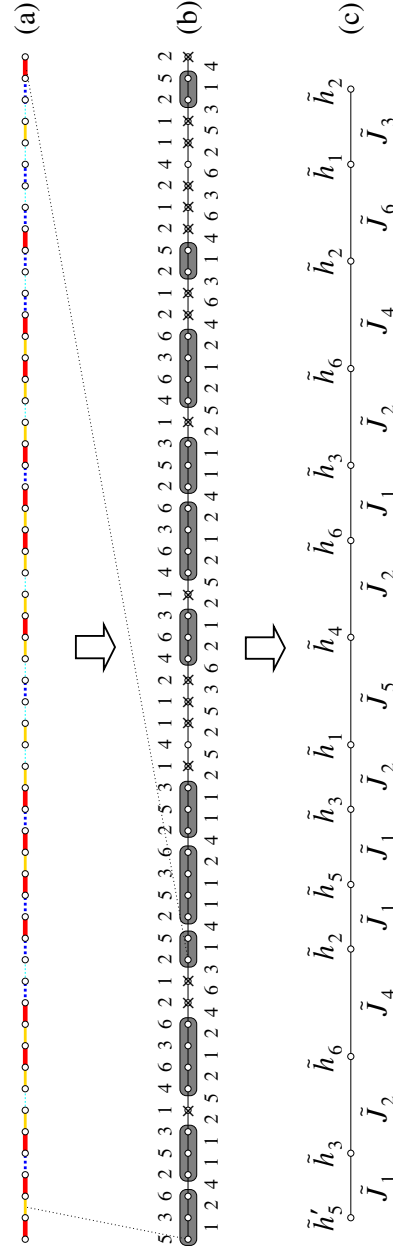


Figure 7: Renormalization-group transformation as applied to the four-letter Rudin-Shapiro chain. The original chain is shown in (a):  $J_a$  bonds are represented by thick solid lines (red);  $J_b$ , by solid lines (yellow);  $J_c$ , by thick dashed lines (blue);  $J_d$ , by thin dashed lines (cyan); open circles mark the position of the spins, under a uniform field  $h \simeq h_{\text{crit}}$ . Spins connected by  $J_a$  or  $J_b$  bonds form clusters, while spins connected only by  $J_c$  or  $J_d$  are decimated. These processes give rise to the effective chain in (b), characterized by 6 different values of both bonds and fields, respectively indicated by the numbers below and above the chain. Upon further lowering of the energy scale, effective spins under the grey boxes cluster together, while crossed circles denote effective spins decimated by the action of strong effective fields. As shown in (c), apart from a minor boundary effect, the next effective chain preserves the structure in (b).

magnetic moments, are given by

$$\begin{aligned}
 J_1 &= J_c, & h_1 &= h^2/J_b, & \mu_1 &= 2, \\
 J_2 &= J_d, & h_2 &= h^2/J_a, & \mu_2 &= 2, \\
 J_3 &= J_c J_d/h, & h_3 &= h^3/J_a J_b, & \mu_3 &= 3, \\
 J_4 &= J_c^2 J_d/h^2, & h_4 &= h^4/J_a J_b^2, & \mu_4 &= 4, \\
 J_5 &= J_c J_d^2/h^2, & h_5 &= h^4/J_a^2 J_b, & \mu_5 &= 4, \\
 J_6 &= J_c^2 J_d^2/h^3, & h_6 &= h^5/J_a^2 J_b^2, & \mu_6 &= 5.
 \end{aligned} \tag{38}$$

As illustrated in Fig. 7(b), weak bonds appear next to strong fields and vice-versa.

Writing again

$$h = h_{\text{crit}} (1 - \delta), \tag{39}$$

which defines  $\delta$  as a measure of the distance to criticality, it can be seen that for  $|\delta| \ll 1$  and  $\rho \ll 1$  the couplings are ordered according to

$$J_1 \simeq h_1 \gg J_2 \simeq h_2 \gg J_3 \simeq h_3 \gg J_4 \simeq h_4 \gg J_5 \simeq h_5 \gg J_6 \simeq h_6.$$

Sufficiently close to the critical point, upon further reduction of the energy scale, this sequence of bonds and fields is mapped onto itself by the bond recursion relations

$$\begin{aligned}
 J_1^{(j+1)} &= J_4^{(j)}, \\
 J_2^{(j+1)} &= J_2^{(j)} J_5^{(j)} / h_1^{(j)}, \\
 J_3^{(j+1)} &= J_2^{(j)} J_3^{(j)} J_5^{(j)} / \left[ h_1^{(j)} \right]^2, \\
 J_4^{(j+1)} &= J_3^{(j)} J_4^{(j)} J_6^{(j)} / h_1^{(j)} h_2^{(j)}, \\
 J_5^{(j+1)} &= J_2^{(j)} J_3^{(j)} J_5^{(j)} J_6^{(j)} / \left[ h_1^{(j)} \right]^2 h_2^{(j)}, \\
 J_6^{(j+1)} &= J_3^{(j)} J_4^{(j)} \left[ J_6^{(j)} \right]^2 / h_1^{(j)} \left[ h_2^{(j)} \right]^2,
 \end{aligned} \tag{40}$$

the field recursion relations corresponding to the dual versions ( $h_i \leftrightarrow J_i$ ) of the above equations, thus defining the RG transformation. We also write recursion relations for the effective magnetic moments,

$$\begin{aligned}
 \mu_1^{(j+1)} &= \mu_4^{(j)}, \\
 \mu_2^{(j+1)} &= \mu_2^{(j)} + \mu_5^{(j)}, \\
 \mu_3^{(j+1)} &= \mu_2^{(j)} + \mu_3^{(j)} + \mu_5^{(j)}, \\
 \mu_4^{(j+1)} &= \mu_3^{(j)} + \mu_4^{(j)} + \mu_6^{(j)}, \\
 \mu_5^{(j+1)} &= \mu_2^{(j)} + \mu_3^{(j)} + \mu_5^{(j)} + \mu_6^{(j)}, \\
 \mu_6^{(j+1)} &= \mu_3^{(j)} + \mu_4^{(j)} + 2\mu_6^{(j)},
 \end{aligned} \tag{41}$$

as well as for the lengths of the effective bonds and fields,

$$\begin{aligned}
 \ell_{J_1}^{(j+1)} &= \ell_{J_4}^{(j)}, \\
 \ell_{J_2}^{(j+1)} &= \ell_{J_2}^{(j)} + \ell_{J_5}^{(j)} + \ell_{h_1}^{(j)}, \\
 \ell_{J_3}^{(j+1)} &= \ell_{J_2}^{(j)} + \ell_{J_3}^{(j)} + \ell_{J_5}^{(j)} + 2\ell_{h_1}^{(j)}, \\
 \ell_{J_4}^{(j+1)} &= \ell_{J_3}^{(j)} + \ell_{J_4}^{(j)} + \ell_{J_6}^{(j)} + \ell_{h_1}^{(j)} + \ell_{h_2}^{(j)}, \\
 \ell_{J_5}^{(j+1)} &= \ell_{J_2}^{(j)} + \ell_{J_3}^{(j)} + \ell_{J_5}^{(j)} + \ell_{J_6}^{(j)} + 2\ell_{h_1}^{(j)} + \ell_{h_2}^{(j)}, \\
 \ell_{J_6}^{(j+1)} &= \ell_{J_3}^{(j)} + \ell_{J_4}^{(j)} + 2\ell_{J_6}^{(j)} + \ell_{h_1}^{(j)} + 2\ell_{h_2}^{(j)},
 \end{aligned} \tag{42}$$

with analogous expressions obtained by interchanging the labels  $J$  and  $h$ . Here,  $l_{J_i}^{(j)}$  or  $l_{h_i}^{(j)}$  represent the length of the effective bond  $J_i$  or field  $h_i$ ,  $i \in \{1, 2, \dots, 6\}$ , at the  $j$ th iteration of the RG transformation.

The recursion relations in Eqs. 40 and their dual counterparts are valid as long as  $h_1^{(j)} > J_2^{(j)}$  and  $J_1^{(j)} > h_2^{(j)}$ . The first condition eventually ceases to be valid in the ferromagnetic phase, while the second one fails in the paramagnetic phase. To be concrete, let us focus on the ferromagnetic phase. From the dual symmetry of the recursion relations (under the interchange of bonds and fields), similar results are valid in the paramagnetic phase.

As in the previous section, it is convenient to introduce a coupling ratio

$$s_1^{(j)} \equiv \frac{J_2^{(j)}}{h_1^{(j)}}, \quad (43)$$

whose value allows us to check the validity of the condition  $h_1^{(j)} > J_2^{(j)}$ . In order to obtain a closed set of recursion relations, it is also necessary to define the additional ratios

$$s_4^{(j)} \equiv \frac{J_5^{(j)}}{h_4^{(j)}}, \quad \text{and} \quad r_i^{(j)} \equiv \frac{h_i^{(j)}}{J_i^{(j)}}, \quad i \in \{1, 2, \dots, 6\}. \quad (44)$$

Substitution of Eqs. 40 into the above expressions, and definition of the ratio

$$t^{(j)} \equiv s_1^{(j)} s_4^{(j)} = s_1^{(j+1)}, \quad (45)$$

lead to a set of recursion relations which in matrix form can be written as

$$\begin{pmatrix} \ln r_1^{(j+1)} \\ \ln r_2^{(j+1)} \\ \ln r_3^{(j+1)} \\ \ln r_4^{(j+1)} \\ \ln r_5^{(j+1)} \\ \ln r_6^{(j+1)} \\ \ln t^{(j+1)} \end{pmatrix} = \begin{pmatrix} 0 & 0 & 0 & 1 & 0 & 0 & 0 \\ 1 & 1 & 0 & 0 & 1 & 0 & 0 \\ 2 & 1 & 1 & 0 & 1 & 0 & 0 \\ 1 & 1 & 1 & 1 & 0 & 1 & 0 \\ 2 & 2 & 1 & 0 & 1 & 1 & 0 \\ 1 & 2 & 1 & 1 & 0 & 2 & 0 \\ -1 & -1 & -1 & 0 & 0 & -1 & 2 \end{pmatrix} \begin{pmatrix} \ln r_1^{(j)} \\ \ln r_2^{(j)} \\ \ln r_3^{(j)} \\ \ln r_4^{(j)} \\ \ln r_5^{(j)} \\ \ln r_6^{(j)} \\ \ln t^{(j)} \end{pmatrix}$$

$$\Rightarrow |v_{j+1}\rangle = \mathbb{T} |v_j\rangle,$$

in a notation analogous to that of Eqs. 17 and 18. From Eqs. 38-45, we see that the initial value of the vector  $|v\rangle$  takes the form

$$|v_0\rangle = \begin{pmatrix} 2 \ln(1 - \delta) \\ 2 \ln(1 - \delta) \\ 4 \ln(1 - \delta) \\ 6 \ln(1 - \delta) \\ 6 \ln(1 - \delta) \\ 8 \ln(1 - \delta) \\ 2 \ln \rho - 8 \ln(1 - \delta) \end{pmatrix}.$$

The eigenvalues of the matrix  $\mathbb{T}$  are  $\lambda_1 = 4$ ,  $\lambda_2 = 2$ ,  $\lambda_3 = \lambda_4 = 1$ , and  $\lambda_5 = \lambda_6 = \lambda_7 = 0$ . Denoting the respective right eigenvectors by  $|\phi_i\rangle$ ,  $i \in \{1, 2, \dots, 7\}$ ,  $|v_0\rangle$  can be expanded as

$$|v_0\rangle = -8 \ln(1 - \delta) |\phi_1\rangle + 2 \ln \rho |\phi_2\rangle - \frac{2}{3} \ln(1 - \delta) |\phi_3\rangle + |w_0\rangle,$$

where  $|w_0\rangle$  belongs to the kernel of  $\mathbb{T}$ . Thus, from  $|v_j\rangle = \mathbb{T}^j |v_0\rangle$  and from explicit expressions for  $|\phi_1\rangle$ ,  $|\phi_2\rangle$  and  $|\phi_3\rangle$ , we obtain, for  $i \in \{1, 2, \dots, 6\}$ ,

$$\begin{cases} \ln r_i^{(j)} &= (f_i \lambda_1^j + g_i \lambda_2^j) \ln(1 - \delta), \\ \ln t^{(j)} &= -8 \lambda_1^j \ln(1 - \delta) + 2 \lambda_2^j \ln \rho, \end{cases}$$

with the constants  $f_i$  and  $g_i$  all positive. It is then clear that at the critical point ( $\delta = 0$ ) we have  $r_i^{(j)} = 1$ , i.e.,  $h_i^{(j)} = J_i^{(j)}$  at all RG steps, whereas  $t^{(j)}$  asymptotically approaches zero. This indicates that the RG scheme becomes asymptotically exact, in agreement with the relevant nature of aperiodic modulations characterized by a wandering exponent  $\omega = \frac{1}{2} > 0$ . Accordingly, the dynamic scaling can be shown to assume the activated form

$$\Omega_j \sim \exp\left(-\sqrt{\ell_j/\ell_\rho}\right),$$

with  $\ell_j$  a characteristic length scale and  $\ell_\rho$  a function of  $\rho$  only. This is exactly the form obeyed by the dynamic scaling behavior of the critical random quantum Ising chain [3, 4].

In the ferromagnetic phase ( $\delta > 0$ ), we have  $r_i^{(j)} < 1$ , as expected, but the RG scheme is no longer valid once  $s_1^{(j)}$  (or equivalently  $t^{(j)}$ ; see Eq. 45) reaches unity. This happens for

$$\ln t^{(j^*)} = 0 \Rightarrow j^* = \frac{\ln \left[ \frac{4 \ln(1-\delta)}{\ln \rho} \right]}{\ln \frac{\lambda_2}{\lambda_1}} \sim \frac{\ln \delta}{\ln(\lambda_2/\lambda_1)}. \quad (46)$$

From this step on we need to redefine the RG transformation, since now  $J_2^{(j)} > h_1^{(j)}$ . It turns out that after one step of this new RG transformation all effective fields are smaller than all effective bonds. Thus, critical properties can be estimated, in the same way as in the previous section, by looking at effective quantities after  $j_\delta \sim j^*$  iterations of the RG scheme.

The matrix connecting effective lengths in consecutive RG steps, built from Eqs. 42 and their dual counterparts, has as its largest eigenvalue  $\lambda_1 = 4$ , so that the correlation length can be estimated as

$$\xi \sim \ell_{j_\delta} \sim \lambda_1^{j_\delta} \sim \delta^{-\nu},$$

with a correlation length exponent

$$\nu = \frac{\ln \lambda_1}{\ln \lambda_1 - \ln \lambda_2} = 2 = \frac{1}{1 - \omega},$$

again saturating the Harris-Luck criterion as written in Eq. 33.

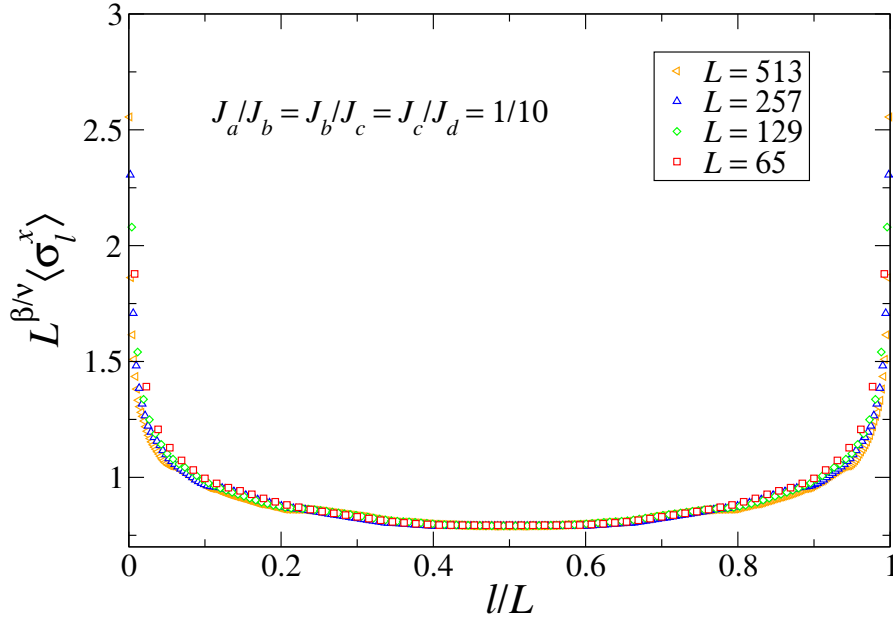


Figure 8: Rescaled average magnetization profiles for the four-letter Rudin-Shapiro sequence, with a coupling ratio  $\rho = \frac{1}{10}$ .

From the recursion relations of the effective magnetic moments, Eq. 41, we similarly extract a characteristic magnetic moment scaling as

$$\mu_j \sim \vartheta_1^j,$$

in which  $\vartheta_1 = 3.24698\dots$  is the largest eigenvalue of the matrix connecting  $\{\mu_i^{(j+1)}\}$  to  $\{\mu_i^{(j)}\}$ . Thus, the spontaneous (bulk) magnetization should scale as

$$m_x \sim \frac{\mu_{j_\delta}}{\ell_{j_\delta}} \sim \left( \frac{\vartheta_1}{\lambda_1} \right)^{j_\delta} \sim \delta^\beta,$$

with a critical exponent

$$\beta = \frac{\ln(\vartheta_1/\lambda_1)}{\ln(\lambda_2/\lambda_1)} = 0.300902\dots$$

In order to check the validity of the above results, we again resort to exact diagonalization of finite chains, based on the free-fermion method. As shown in Fig. 8, these calculations are fully compatible with the above prediction for the ratio  $\beta/\nu$ . Notice that now there is a clear collapse of the curves only for the bulk magnetization, and the presence of four rather than two distinct bond leads to the disappearance of the second master curve visible in Fig. 4.

## 5.2. The two-letter sequence

The results derived in the previous subsection are valid as long as the four bonds assume distinct values. However, by making the identifications  $J_b \equiv J_a$  and  $J_d \equiv J_c$  we obtain a binary RS sequence, and the properties of the corresponding quantum Ising chain can

in principle be different. For instance, numerical calculations and scaling considerations based on a mapping to a directed walk led Iglói *et al.* [12] to propose for this binary sequence a correlation-length critical exponent  $\nu = 4/3$  and a ratio  $\beta/\nu = 0.160$  (5).

For the quantum Ising chain with couplings following the binary RS sequence, with  $J_a = \rho J_c$ ,  $0 < \rho < 1$ , the critical field is given by

$$h_{\text{crit}} = \rho^{\frac{1}{2}} J_c.$$

When applying the SDRG scheme, we thus focus on the condition  $J_a \ll h \ll J_c$ . As shown in Fig. 9(a), the original chain has clusters with 1 to 4 strong bonds. At energy scales  $\Omega$  such that  $J_a < h < \Omega < J_c$ , this gives rise to 4 different effective magnetic moments  $\{\mu_n\}$  and fields  $\{h_n\}$ , with

$$\mu_n = (n+1)\mu \quad \text{and} \quad h_n = \frac{h^{n+1}}{J_c^n}, \quad n \in \{1, 2, 3, 4\}. \quad (47)$$

At this point, all bonds are equal to  $J_a$ , and the largest energy scale in the chain is provided by the original fields  $h$ . Thus, at energy scales such that  $J_a < \Omega < h$ , all spins under the action of  $h$  can be decimated, inducing 4 different effective bonds

$$J_n = \frac{J_a^n}{h^{n-1}}, \quad n \in \{1, 2, 3, 4\}. \quad (48)$$

The resulting effective chain is depicted in Fig. 9(b), and corresponds to a sequence of 4 different bonds and fields.

Exactly at the critical point, the bonds and fields are ordered such that

$$J_1 = h_1 > J_2 = h_2 > J_3 = h_3 > J_4 = h_4,$$

with

$$J_n = \rho^{\frac{n+1}{2}} J_c.$$

Notice from Fig. 9(b) that now, contrary to what happens for the four-letter RS chain, there are clusters of 1 to 3 strong bonds  $J_1$  or fields  $h_1$ , and in some of these clusters both strong bonds and strong fields are present. Of course, this picture remains valid in the neighborhood of the critical point, making it harder to write recursion relations, since the perturbative treatment becomes more involved. However, we can take advantage of a mapping between the critical quantum Ising chain and the quantum  $XX$  chain [35] and of the results derived for the aperiodic quantum  $XX$  chain (see Ref. [24]) to write the bond recursion relations

$$\begin{aligned} J_1^{(j+1)} &= f(J_1^{(j)}, h_1^{(j)}) J_1^{(j)} J_3^{(j)}, \\ J_2^{(j+1)} &= \left[ f(J_1^{(j)}, h_1^{(j)}) \right]^2 \left[ J_1^{(j)} \right]^2 J_2^{(j)} J_3^{(j)} / h_1^{(j)}, \\ J_3^{(j+1)} &= f(J_1^{(j)}, h_1^{(j)}) J_1^{(j)} J_2^{(j)} J_3^{(j)} J_4^{(j)} / \left[ h_1^{(j)} \right]^2, \\ J_4^{(j+1)} &= J_2^{(j)} J_3^{(j)} \left[ J_4^{(j)} \right]^2 / \left[ h_1^{(j)} \right]^3 \end{aligned} \quad (49)$$

with dual recursion relations for the effective fields, the function  $f(J, h)$  being explicitly given by

$$f(J, h) = (J^2 + h^2)^{-\frac{1}{2}}.$$

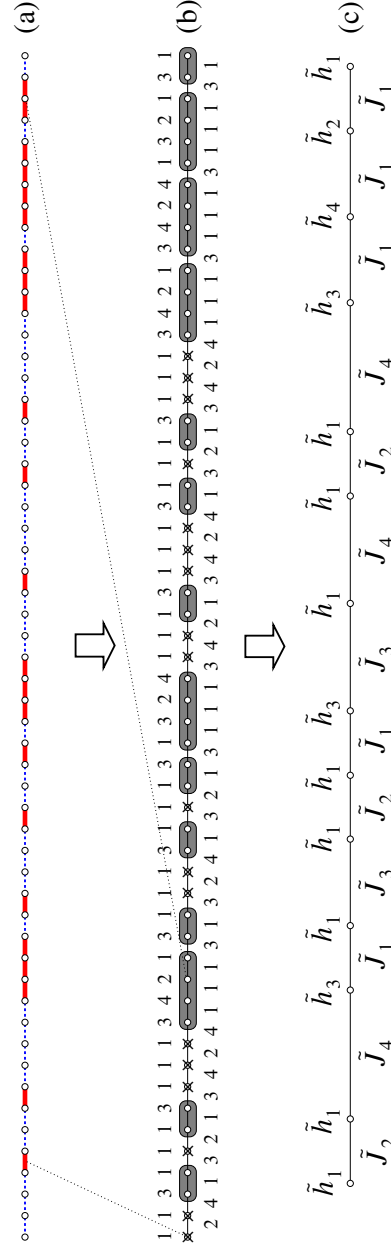


Figure 9: Renormalization-group transformation as applied to the two-letter Rudin-Shapiro chain. The original chain is shown in (a):  $J_a$  bonds are represented by dashed lines (blue), while stronger  $J_c$  bonds appear as solid lines (red); open circles mark the position of the spins, under a uniform field  $h \simeq h_{\text{crit}}$ . Spins connected by  $J_c$  bonds form clusters, while spins connected only by  $J_a$  are decimated. These processes give rise to the effective chain in (b), characterized by 4 different values of both bonds and fields, respectively indicated by the numbers below and above the chain. Upon further lowering of the energy scale, effective spins under the grey boxes cluster together, while crossed circles denote effective spins decimated by the action of strong effective fields. As shown in (c) the next effective chain preserves the structure in (b).

The above recursion relations define an RG transformation which maps the effective chain onto itself as long as

$$J_1^{(j)} > h_2^{(j)} \quad \text{and} \quad h_1^{(j)} > J_2^{(j)}. \quad (50)$$

Recursion relations for the lengths of the effective couplings take the form

$$\begin{aligned} \ell_{J_1}^{(j+1)} &= \ell_{J_3}^{(j)}, \\ \ell_{J_2}^{(j+1)} &= \ell_{J_2}^{(j)} + \ell_{J_3}^{(j)} + \ell_{h_1}^{(j)}, \\ \ell_{J_3}^{(j+1)} &= \ell_{J_2}^{(j)} + \ell_{J_3}^{(j)} + \ell_{J_4}^{(j)} + 2\ell_{h_1}^{(j)}, \\ \ell_{J_4}^{(j+1)} &= \ell_{J_2}^{(j)} + \ell_{J_3}^{(j)} + 2\ell_{J_4}^{(j)} + 3\ell_{h_1}^{(j)}, \\ \ell_{h_1}^{(j+1)} &= \ell_{h_1}^{(j)} + \ell_{h_3}^{(j)} + \ell_{J_1}^{(j)}, \\ \ell_{h_2}^{(j+1)} &= 2\ell_{h_1}^{(j)} + \ell_{h_2}^{(j)} + \ell_{h_3}^{(j)} + 3\ell_{J_1}^{(j)}, \\ \ell_{h_3}^{(j+1)} &= \ell_{h_1}^{(j)} + \ell_{h_2}^{(j)} + \ell_{h_3}^{(j)} + \ell_{h_4}^{(j)} + 3\ell_{J_1}^{(j)}, \\ \ell_{h_4}^{(j+1)} &= \ell_{h_2}^{(j)} + \ell_{h_3}^{(j)} + 2\ell_{h_4}^{(j)} + 3\ell_{J_1}^{(j)}, \end{aligned} \quad (51)$$

with the initial values  $\ell_{J_1}^{(0)} = \frac{1}{2}$ ,  $\ell_{J_2}^{(0)} = \ell_{h_1}^{(0)} = \frac{3}{2}$ ,  $\ell_{J_3}^{(0)} = \ell_{h_2}^{(0)} = \frac{5}{2}$ ,  $\ell_{J_4}^{(0)} = \ell_{h_3}^{(0)} = \frac{7}{2}$ ,  $\ell_{h_4}^{(0)} = \frac{9}{2}$ .

At the critical point,  $f(J_1^{(j)}, h_1^{(j)})$  reduces to  $f(J_1^{(j)}, J_1^{(j)}) = 1/\sqrt{2}J_1^{(j)}$ , and the recursion relations in Eqs. 49 recover the multiplicative structure satisfied by the previously discussed aperiodic chains. Then, we can show by the method described for the four-letter RS sequence that again the SDRG approach becomes asymptotically exact, predicting a dynamic scaling form

$$\Omega_j \sim \exp\left(-\sqrt{\ell_j/\ell_\rho}\right),$$

consistent with the value  $\omega = \frac{1}{2}$  of the wandering exponent of the binary RS sequence.

The analytical treatment of the recursion relations in the off-critical regime is hindered by the presence of the function  $f(J, h)$ . It is possible to perform an expansion on the distance  $\delta$  to criticality in order to determine at which step of the RG transformation the condition in Eq. 50 ceases to be valid. However, not only is the resulting equation impossible to solve in closed form, but also the new RG transformation which we have to impose does not seem to lead to an invariant sequence of effective couplings. Thus, we have to recourse to a numerical implementation of the SDRG scheme.

In order to reach the largest possible system sizes, we start at a given distance to criticality  $\delta$  (defined as in Eq. 39) and apply the recursion relations 49 (and their dual counterparts) up to the point at which  $\min\{J_1^{(j)}, h_1^{(j)}\} < \max\{J_2^{(j)}, h_2^{(j)}\}$ , keeping track of the effective lengths via Eqs. 51. Let us denote the effective couplings at this point by  $\{J_n^{(j*)}\}$  and  $\{h_n^{(j*)}\}$ . Since up to this point the sequence of effective couplings is invariant under the RG transformation, it can be generated by applying the rules leading to Eqs. 47 and 48 to a chain with bonds following the binary RS sequence. To the resulting effective couplings, we then assign the values  $\{J_n^{(j*)}\}$  and  $\{h_n^{(j*)}\}$ , and iterate numerically the SDRG scheme by sweeping through the lattice and progressively eliminating the high-energy degrees of freedom. For a binary RS sequence

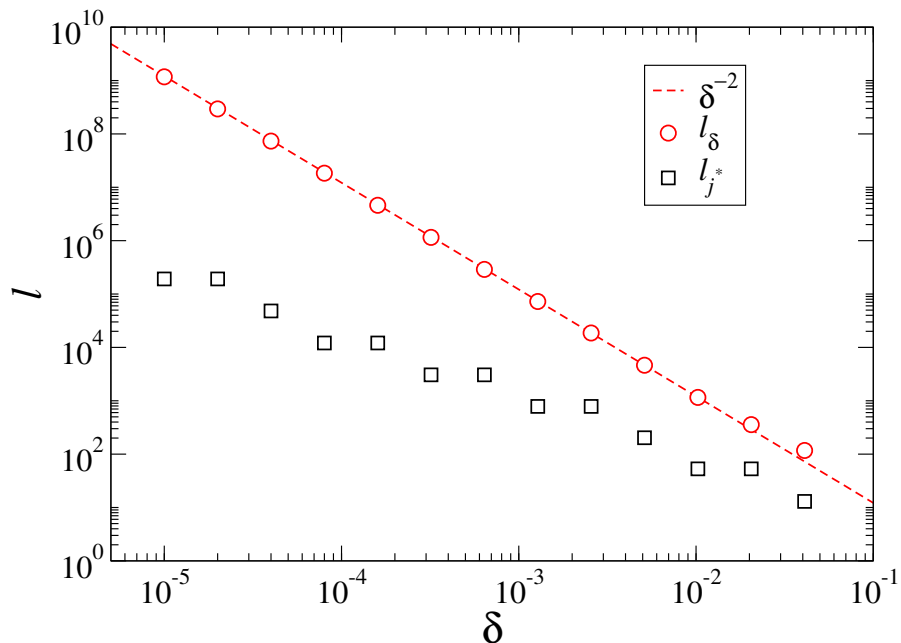


Figure 10: Dependence of the lengths  $\ell_\delta$  (proportional to the correlation length) and  $\ell_{j^*}$  on the distance to criticality  $\delta$ , for a coupling ratio  $J_a/J_c = \frac{1}{2}$ .

with  $2^{20} \simeq 10^6$  letters, the corresponding number of  $\{J_n\}$  and  $\{h_n\}$  couplings is around  $5 \times 10^5$ , and correcting for the lengths of the effective couplings leads to a real chain containing  $6 \times 10^{12}$  spins for  $\delta = 10^{-5}$ .

We implement this numerical procedure, in the paramagnetic phase, up to the point at which all bonds become smaller than all fields. In Fig. 10 we plot, for  $\rho = \frac{1}{2}$ , the scaling behavior of the length  $\ell_\delta$  of the strongest bond at that point, as a function of the distance to criticality. Also shown is the length  $\ell_{j^*}$  of the strongest bond  $J_1^{(j^*)}$  at the point beyond which the sequence of effective lengths is no longer invariant. We see that  $\ell_\delta$  nicely follows a power law  $\ell_\delta \sim |\delta|^{-2}$ , and thus we conclude that, using  $\ell_\delta$  as an estimate of the correlation length, we obtain

$$\xi \sim |\delta|^{-\nu},$$

with an exponent  $\nu = 2$ .

This result is in contrast to that obtained by Iglói et al. from a scaling argument for the surface magnetization of finite chains, based on an equivalence of the problem with a directed walk. As already mentioned, these authors predict a correlation-length critical exponent  $\nu = \frac{4}{3}$ . They also provide an estimate of the ratio  $\beta/\nu \simeq 0.160$ , by adjusting numerical results for critical magnetization profiles of small chains (containing between 9 and 65 spins), with a ratio between weak and strong bonds given by  $J_a/J_c = 1/16$ . Incidentally, they find the surprising result that the data for such small chains can be well fitted by the predictions of conformal invariance, although the system is clearly not conformally invariant, in view of the strongly anisotropic scaling along the space and time directions.

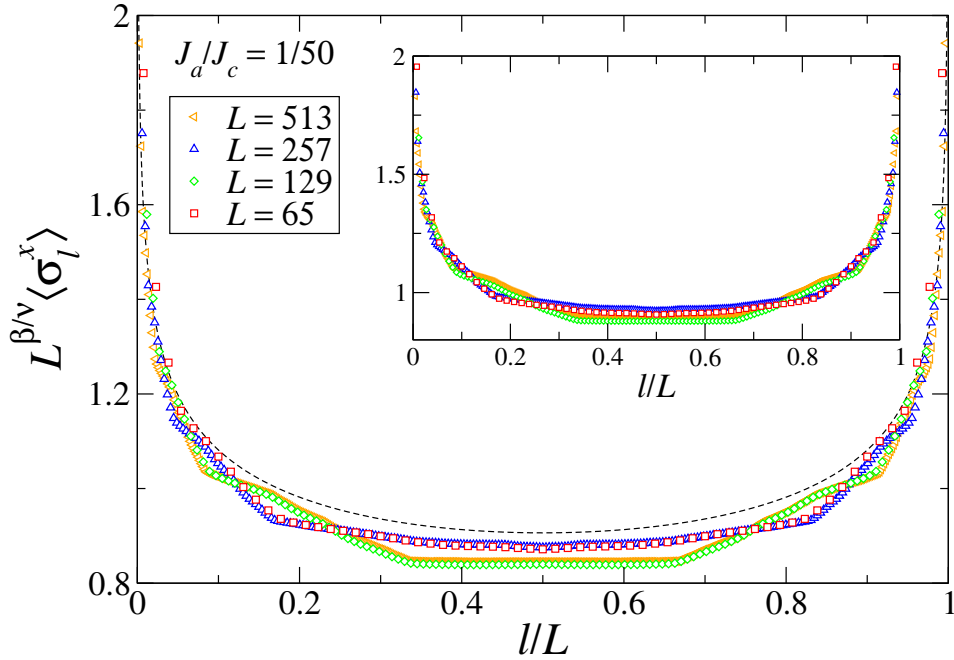


Figure 11: Rescaled average magnetization profiles for the two-letter Rudin-Shapiro quantum Ising chain. Main panel: rescaling with the exponents calculated by the SDRG approach. Inset: rescaling with the numerical estimate of Ref. [12]. The dashed line in the main panel corresponds to the conformal-invariance prediction, Eq. 52.

We then decided to use the free-fermion method to look at larger chain sizes, and smaller bond ratios, in order to check whether we could fit the numerical results with our prediction for  $\beta/\nu$ , assuming, on the grounds of universality, that the ratio  $\beta/\nu = 0.150451\dots$  found for the four-letter RS chain would still be valid for the two-letter RS chain. Figure 11 shows the results of free-fermion calculations of critical magnetization profiles for chains containing between 65 and 513 spins, and  $J_a/J_c = 1/50$ . Despite the small difference between our prediction for  $\beta/\nu$  and that of Ref. [12], the inset shows that our prediction yields a better data collapse. Although the results shown in Fig. 11 are definitely incompatible with the conformal-invariance form

$$m_x(l/L) \sim [L \sin(\pi l/L)]^{-\beta/\nu}, \quad (52)$$

we do observe a reasonable agreement with such form for small chains (not shown), as in Ref. [12]. This agreement becomes poorer as the coupling ratio is reduced.

Furthermore, the results in Eqs. 28 and 34 can be used to check directly the prediction  $\nu = 2$ , from free-fermion calculations of the lowest gap  $\Omega_L(\delta)$  for chains with  $L$  spins, at a distance  $\delta$  from criticality, via the finite-size scaling *ansatz*

$$-\ln \Omega_L(\delta) = L^\omega f(\delta L^{1/\nu}),$$

in which  $f(x)$  is a scaling function predicted to behave as

$$f(x) \sim x^{-\omega\nu}$$

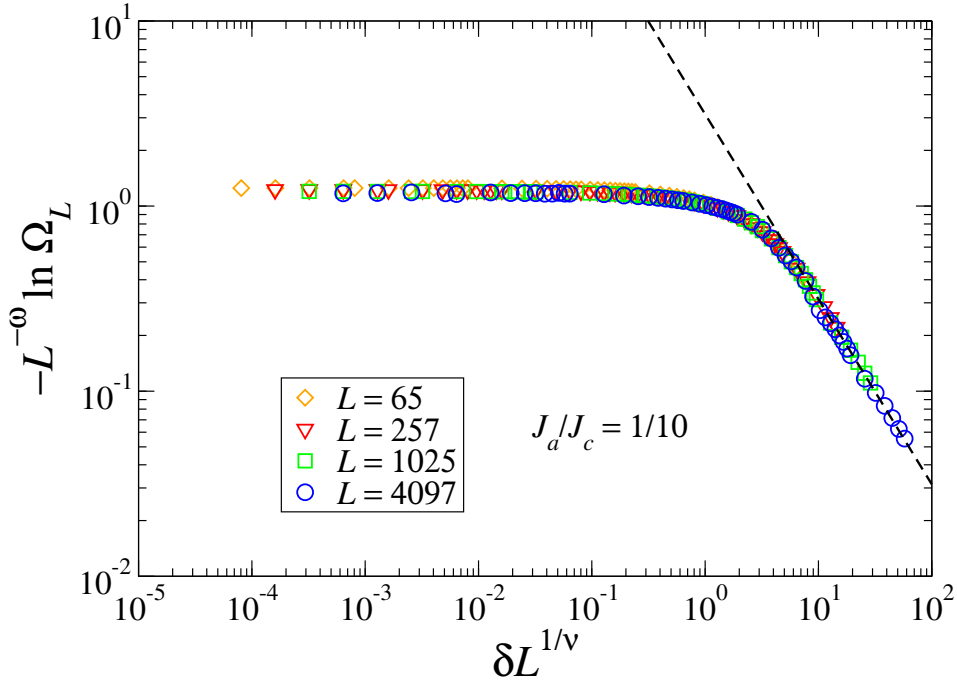


Figure 12: Finite-size scaling plot of the lowest gap calculated numerically for off-critical quantum Ising chains with couplings following the binary Rudin-Shapiro sequence. Parameters correspond to  $\omega = \frac{1}{2}$  and  $\nu = 2$ . The dashed line is proportional to  $(\delta L^{1/\nu})^{-\omega\nu}$ .

for  $x \gg 1$ . As seen in Fig. 12, we obtain very good data collapse for binary Rudin-Shapiro chains with coupling ratio  $J_a/J_c = 1/10$ , and lengths ranging from  $L - 1 = 64$  to  $L - 1 = 4096$ , by setting  $\omega = \frac{1}{2}$  and using the SDRG prediction  $\nu = 2$ .

## 6. Discussion and conclusions

In this paper, we have presented an extension of the strong-disorder renormalization group approach for the study of the low-energy critical behavior of the quantum Ising chain with couplings chosen from aperiodic but deterministic sequences, generated by substitution rules.

For the cases of marginal and relevant aperiodicity, in which the critical behavior is expected to depart from the Onsager universality class, we have been able to obtain analytical results for various critical exponents, such as those related to the correlation length, the bulk magnetization, and the spin-spin correlation functions at criticality. Interestingly, we always find that the correlation-length critical exponent is given by  $\nu = (1 - \omega)^{-1}$ , a result which barely satisfies the Harris-Luck criterion [10, 19] around the aperiodic fixed point, which takes the form  $\nu \geq (1 - \omega)^{-1}$ . We have also derived results for the off-critical lowest energy gaps, which reflect the absence of Griffiths singularities for the present class of aperiodic systems, as expected from previous arguments [12, 25]. All our results have been fully confirmed by numerical calculations on finite chains,

based on the free-fermion methods.

The basic physical picture offered by the SDRG approach, derived for a family of two-letter substitution rules, has been shown to remain valid for more complicated sequences, represented by the two- and four-letter Rudin-Shapiro sequences. According to this picture, sufficiently close to the critical point, as the energy scale is progressively reduced, the effective chains generated along the RG process exhibit a self-similar structure, in which the sequence of effective couplings remains invariant and their values decrease, whereas the magnetic moments of the effective spins and the distances between those spins grow exponentially. This picture holds up to a certain step of the RG process, beyond which the ground-state of the chain settles into either the ferromagnetic or the paramagnetic phases, characterized respectively by the dominance of bonds or fields.

The self-similar nature of the effective chains is helpful in understanding the absence of Griffiths singularities in the systems studied here. At all length scales, self-similarity guarantees that geometric fluctuations are entirely governed by the wandering exponent  $\omega$ , setting a maximum size for locally critical clusters, as already noted in [25]. This is in contrast with the uncorrelated random quantum Ising chain, where the wandering exponent only gauges the growth of average geometric fluctuations, there being a nonzero probability for the occurrence of arbitrarily large clusters of spins which are locally in a different phase than the bulk.

Finally, the results reported here, concerning critical exponents and the nature of the ground state phases, remain valid for aperiodic XY chains, described by the Hamiltonian

$$\mathcal{H} = -\frac{1}{2} \sum_i J_i [(1 + \gamma_i) \sigma_i^x \sigma_{i+1}^x + (1 - \gamma_i) \sigma_i^y \sigma_{i+1}^y] - \sum_i h_i \sigma_i^z,$$

as long as the anisotropy parameters  $\gamma_i$ ,  $0 \leq |\gamma_i| \leq 1$ , are all positive or all negative. Under these conditions, the SDRG scheme is straightforwardly adapted, and it can be shown [36] that the anisotropies  $\gamma_i$  flow towards  $|\tilde{\gamma}_i| = 1$  as the RG scheme is iterated, so that the low-energy behavior corresponds to that of the quantum Ising chain.

## Acknowledgments

We thank J. A. Hoyos for useful conversations and a critical reading of the manuscript. This work has been supported by the Brazilian agencies CNPq and FAPESP.

- [1] Ma S K, Dasgupta C and Hu C K 1979 *Phys. Rev. Lett.* **43** 1434
- [2] Dasgupta C and Ma S K 1980 *Phys. Rev. B* **22** 1305
- [3] Fisher D S 1992 *Phys. Rev. Lett.* **69** 534
- [4] Fisher D S 1995 *Phys. Rev. B* **51** 6411
- [5] Griffiths R B 1969 *Phys. Rev. Lett.* **23** 17
- [6] Schechtman D, Blech I, Gratias D and Cahn J W 1984 *Phys. Rev. Lett.* **53** 1951
- [7] Luck J M 1993 *J. Stat. Phys.* **72** 417
- [8] Iglói F, Turban L, Karevski D and Szalma F 1997 *Phys. Rev. B* **56** 11031

- [9] Hermisson J, Grimm U and Baake M 1997 *J. Phys. A: Math. Gen.* **30** 7315
- [10] Luck J M 1993 *Europhys. Lett.* **24** 359
- [11] Iglói F, Karevski D and Rieger H 1998 *Eur. Phys. J. B* **1** 513
- [12] Iglói F, Karevski D and Rieger H 1998 *Eur. Phys. J. B* **5** 613
- [13] Szállás A 2005 Diplomathesis, University of Szeged
- [14] Iglói F, Juhász R and Zimborás Z 2007 *Europhys. Lett.* **79** 37001
- [15] McCoy B and Wu T T 1968 *Phys. Rev.* **176** 631
- [16] McCoy B and Wu T T 1971 *The Two-dimensional Ising Model* (Harvard University Press)
- [17] Iglói F 2002 *Phys. Rev. B* **65** 064416
- [18] Pfeuty P 1979 *Phys. Lett. A* **72** 245
- [19] Harris A B 1974 *J. Phys. C* **7** 1671
- [20] Grimm U and Baake M 1997 Aperiodic Ising models *The mathematics of long-range aperiodic order* NATO ASI Series C 489 ed Moody R V (Kluwer) p 199
- [21] Kogut J 1979 *Rev. Mod. Phys.* **51** 659
- [22] Hoyos J A, Laflorigie N, Vieira A P and Vojta T 2011 *Europhys. Lett.* **93** 30004
- [23] Vieira A P 2005 *Phys. Rev. Lett.* **94** 077201
- [24] Vieira A P 2005 *Phys. Rev. B* **71** 134408
- [25] Hermisson J 2000 *J. Phys. A: Math. Gen.* **33** 57
- [26] Fisher D S 1999 *Physica A* **263** 222
- [27] Chayes J T, Chayes L, Fisher D S and Spencer T 1986 *Phys. Rev. Lett.* **57** 2999
- [28] Barouch E and McCoy B 1971 *Phys. Rev. A* **3** 786
- [29] Katsura S 1962 *Phys. Rev.* **127** 1508
- [30] Pfeuty P 1970 *Ann. Phys.* **57** 79
- [31] Iglói F and Rieger H 1998 *Phys. Rev. B* **57** 11404
- [32] Guttmann A J 1989 Asymptotic analysis of power-series expansions *Phase Transitions and Critical Phenomena* vol 13 ed Domb C and Lebowitz J L (Academic Press, London)
- [33] Burkhardt T W and Eisenriegler E 1985 *J. Phys. A: Math. Gen.* **18** L83
- [34] Iglói F, Peschel I and Turban L 1993 *Adv. Phys.* **42** 683
- [35] Fisher D S 1994 *Phys. Rev. B* **50** 3799
- [36] de Oliveira Filho F J 2011 *Efeitos da aperiodicidade sobre as transições quânticas em cadeias XY* Master's thesis Instituto de Física, Universidade de São Paulo